### 14 Neutrino experiments

In the following we discuss how the values of the **PMNS** matrix elements are extracted from data. The first experiments were "disappearance" experiments where one measured the neutrino flux of a given flavour near the emission point and compared it to the flux of neutrinos of the same flavour measured at a distance. More recently several collaborations are able to carry out "appearance" experiments where one measures, near or far from the emission point, the flux of neutrino of a flavour different from the emitted one.

The source of (anti)neutrinos are varied:

- Nuclear reactors produce  $\overline{\nu}_e$  of typical energy  $\langle E_{\overline{\nu}_e} \rangle \approx 3$ . MeV which are measured close to the reactors  $\sim 100$  m or  $\sim 1$  km (Double Chooz, Daya Bay, RENO) or far away 180 km (KAMLAND).
- At accelerators,  $\pi^{\pm}$ 's produced in hadronic collisions decay predominently in  $\nu_{\mu}$  and  $\overline{\nu}_{\mu}$  while  $K^{\pm}$ 's decay also  $\nu_{e}$  and  $\overline{\nu}_{e}$ . The average energy  $\langle E_{\nu} \rangle \approx 1$  GeV and the flux is measured at a distance of 295 km (T2K), 735 km (MINOS), 810 km (NO $\nu$ A). For OPERA the incident neutrino energy is much higher  $\langle E_{\nu_{\mu}} \rangle \approx 17$  GeV and the detector is 730 km away from the source. All these are long baseline experiments.
- Atmospheric neutrinos are produced in cosmic ray showers from  $\pi^+ \to \nu_\mu \, \mu^+$  followed by  $\mu^+ \to e^+ \, \nu_e \, \overline{\nu}_\mu$  (and similarly with  $\pi^-$ ) so that they are a mixture  $(\nu_\mu + \overline{\nu}_\mu)$  and  $(\nu_e + \overline{\nu}_e)$  in proportion 2: 1 at low energy < 1 Gev. Before being detected the neutrinos travel 1 to 30 km (above the Earth, "downward flux") or  $1.3 \, 10^4$  km (through the Earth, "upward flux") (SNO, Super-Kamiokande).
- For the solar neutrinos, the flux from  $^8$ B ( $^8$ B  $\rightarrow ^7$ Be\*  $+ e^+ + \nu_e$ ) is particularly useful. It has a relatively large energy, 1.5 MeV  $< E_{\nu} < 15$  MeV, and the  $^8$ B is the only source of  $\nu_e$ 's in this energy range. The neutrinos travel 1.5 10<sup>8</sup> km before being detected in mines on Earth (SNO). Previous experiments (GALLEX, GNO, SAGE) measured the flux of lower energy  $\nu_e$ 's: .1 MeV  $< E_{\nu} < .4$  MeV.
- Ultra-high energy or cosmic or cosmogenic neutrinos have energies in the range of 100 TeV to several PeV: they are produced by collisions of ultra-high energy cosmic rays on protons or photons, for example on photons from the Cosmic Microwave Background (CMB), and by

sources such as Active Galactic Nuclei (AGN). Their flux is very small and they require huge detectors (telescopes) to be observed (IceCube, ANTARES, KM3net, Baikal-GVD).

#### 14.1 Nuclear reactors: KamLAND, Double-Chooz, Daya Bay, RENO

Nuclear reactors produce dominantly electron antineutrinos and, assuming three flavours, we recall that their survival probability at a distance x is from eq. (12.25),

$$P(\overline{\nu}_e \to \overline{\nu}_e) = 1 - \sin^2(2\theta_{12}) \cos^4(\theta_{13}) \sin^2(\delta m_{21}^2 x/4 k)$$
$$- \sin^2(2\theta_{13}) \sin^2(\theta_{12}) \sin^2(\delta m_{32}^2 x/4 k)$$
$$- \sin^2(2\theta_{13}) \cos^2(\theta_{12}) \sin^2(\delta m_{31}^2 x/4 k). \tag{14.1}$$

## 14.1.1 Long baseline: KamLAND, $\delta m_{21}^2$ , $\theta_{12}$

KamLAND, a long baseline experiment (< x>=180 km) with the detector in Kamioka mine in Gifu, Japan, receives  $\overline{\nu}_e$ 's from 56 nuclear power reactors<sup>48</sup>. The average neutrino energy is < k>=3. MeV so that the factors  $x \, \delta m_{31}^2/4 < k> \approx x \, \delta m_{32}^2/4 < k> \approx 190$ , and integrating over the energy of the neutrino, averages the value of the factors  $\sin^2(x \, \delta m_{31}^2/4k) \approx \sin^2(x \, \delta m_{32}^2/4k) \approx 0.5$ . The equation above reduces to

$$P(\overline{\nu}_e \to \overline{\nu}_e) \approx 1 - \cos^4(\theta_{13}) \sin^2(2\theta_{12}) \sin^2(\delta m_{21}^2 x/4 k) - 0.5 \sin^2(2\theta_{13})$$
$$\approx \cos^4(\theta_{13}) P^{(2)}(\overline{\nu}_e \to \overline{\nu}_e) + \sin^4(\theta_{13})$$
(14.2)

where one has introduced the oscillation probability in a two flavour neutrino world, eq. (12.43),

$$P^{(2)}(\overline{\nu}_e \to \overline{\nu}_e) = 1 - \sin^2(2\theta_{12}) \sin^2(\delta m_{21}^2 x/4 k). \tag{14.3}$$

Taking advantage of the smallness of  $\sin^2(\theta_{13})$ , it is reasonable to make the further approximation (appropriate for long baseline experiments), neglecting  $\sin^4(\theta_{13})$  terms,

$$P(\overline{\nu}_e \to \overline{\nu}_e) \approx (1 - 2\sin^2(\theta_{13})) P^{(2)}(\overline{\nu}_e \to \overline{\nu}_e)$$
(14.4)

The survival probability plotted, in fig. 8, as a fonction of  $L_0/E_{\overline{\nu}_e} = x/k$  in our notation is clearly seen in the figure from the KamLAND collaboration. One observes that the 2-neutrino best fit is very similar to the 3-neutrino one, meaning a very small value for  $\theta_{13} \sim 0$ . Using the 3-neutrino analysis they obtain<sup>49</sup>:

$$\delta(m_{21}^2) = (7.54 + {}^{0.19}_{-0.18}) \ 10^{-5} \ \text{eV}^2, \qquad \sin^2(\theta_{12}) = 0.325 + {}^{0.045}_{-0.039} \ . \tag{14.5}$$

<sup>&</sup>lt;sup>48</sup>KamLAND collaboration, A. Gando *et al.*, Phys.Rev **D83** (2011) 052002, arXiv:1009.4771, [hep-ex].

<sup>&</sup>lt;sup>49</sup>Atsuto Suzuki, Eur.Phys.J. **C74** (2014) 3094, arXiv:1409.4515 [hep-ex].

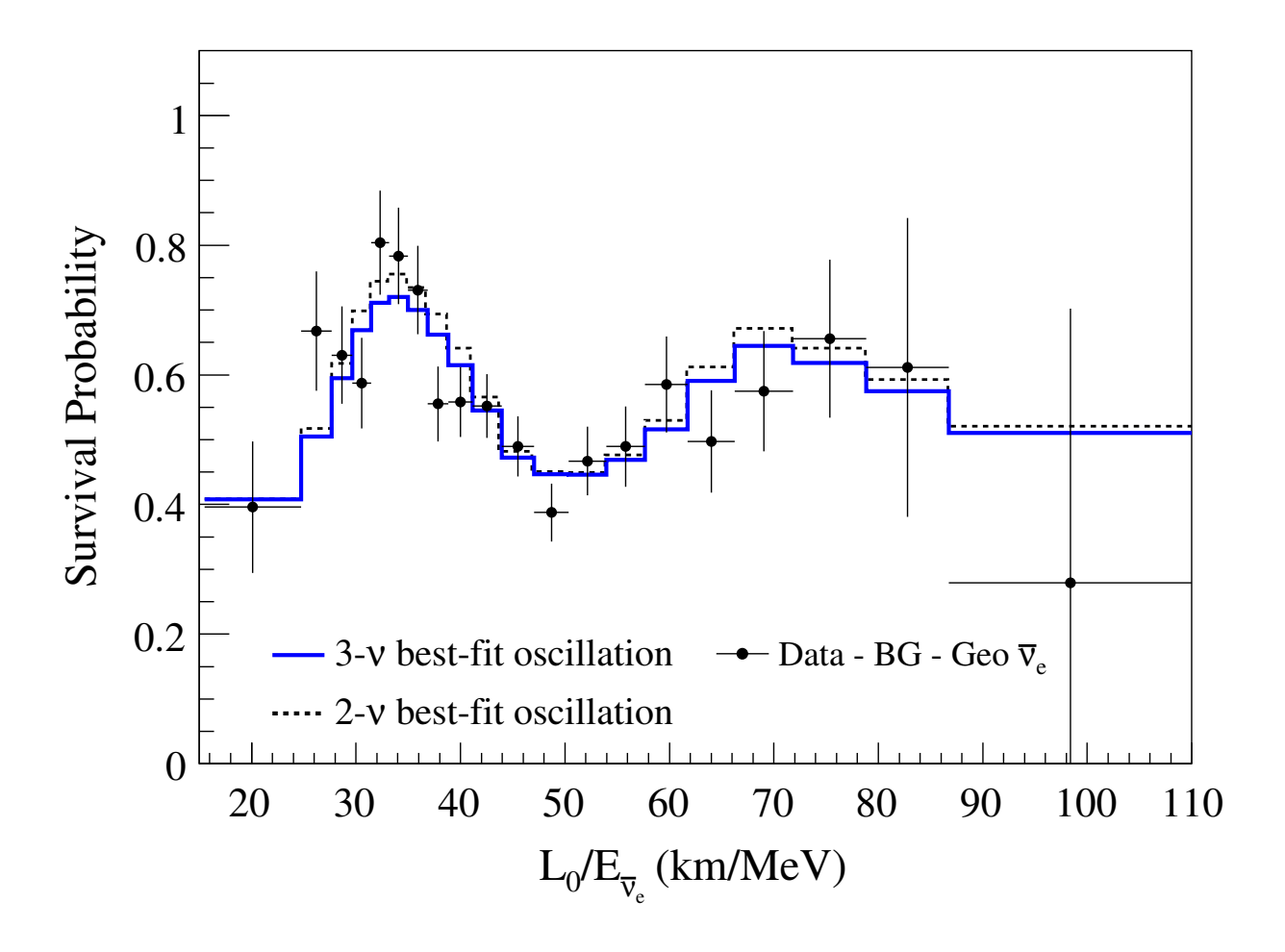


Figure 8: KamLAND oscillation pattern and fits in the 2- $\nu$  and 3- $\nu$  models.

# 14.1.2 Short baseline: Double-Chooz, Daya Bay, RENO, $\delta m_{31}^2, \, \theta_{13}$

Double-Chooz<sup>50</sup>, Daya Bay<sup>51</sup> and RENO<sup>52</sup> are short baseline experiments. They have near detectors at a distance of typically 300 m to 600 m and far detectors at a distance of typically 1000 m to 1700 m. In these configurations the  $\delta m_{21}^2$  term in eq. (14.1) becomes negligible and the oscillations are dominated by  $\delta m_{31}^2 \approx \delta m_{32}^2$  terms so that the probability function reduces to (appropriate for short baseline experiments):

$$P(\overline{\nu}_e \to \overline{\nu}_e) \approx 1 - \sin^2(2\theta_{13}) \sin^2(\delta m_{32}^2 x/4k). \tag{14.6}$$

<sup>&</sup>lt;sup>50</sup>Double-Chooz collaboration, C. Buck, PoS NEUTEL2015 (2015) 015.

<sup>&</sup>lt;sup>51</sup>Daya Bay collaboration, D. Aday *et al.*, Phys. Rev. Lett. **121** (2018) 241805, arXiv:1809.02261 [hep-ex]; they use the complete expression eq. (14.1) in their fit to data.

<sup>&</sup>lt;sup>52</sup>RENO collaboration, G. Bak *et al.*, Phys. Rev. Lett. **121** (2018) 201801, arXiv:1806.00248 [hep-ex].

With the high statistics available these short baseline experiments are well suited to constrain the small  $\theta_{13}$  mixing angle. For instance, the Daya Bay collaboration reports a precise determination of the angle  $\theta_{13}$ ,  $\sin^2 2\theta_{13} = 0.0856 \pm 0.0029$ . They also quote the value for the mass-squared difference for normal ordering  $\delta m_{32}^2 = (2.471^{+.0068}_{-.0070}) \ 10^{-3} \ \text{eV}^2$ . Recently the result from Double Chooz<sup>53</sup> is  $\sin^2 2\theta_{13} = 0.105 \pm 0.0014$ .

# 14.2 Neutrinos from accelerators: T2K, NO $\nu$ A and OPERA; $\delta m_{32}^2$ , $\theta_{23}$ , $\delta$

T2K is a long baseline experiment with a muon neutrino beam with a peak energy of 0.6 GeV produced at the J-PARC (Japan Proton Accelerator Research Complex in Tokai) facility and observed in a near detector at 280 m and in the Super-Kamiokande detector at a distance x=295 km from the production source. This is both a  $\nu_{\mu}$  disappearance and a  $\nu_{e}$  appearance experiment. In 2011 the collaboration gave the first indication of  $\nu_{e}$  appearance in a  $\nu_{\mu}$  beam<sup>54</sup>. Based on the small number of  $\nu_{e}$  observed, a non vanishing value of  $\theta_{13}$  is obtained for the first time:  $\sin \theta_{13} = .11$  with a large error however. Results analysing both  $\nu$  and  $\overline{\nu}$  oscillations based on a  $\nu_{\mu}$  beam generated by 7.48 10<sup>20</sup> POT ("protons on target") and a  $\overline{\nu}_{\mu}$  beam from 7.47 10<sup>20</sup> POT have been published in 2017<sup>55</sup>. Comparing  $\nu_{\mu} \rightarrow \nu_{e}$  and  $\overline{\nu}_{\mu} \rightarrow \overline{\nu}_{e}$  transitions is very useful to extract a precise measurement of the  $\mathcal{CP}$  violating parameter. In a simplified form  $(\delta m_{31}^2 = \delta m_{32}^2)$ , the  $\nu_{\mu}$  survival probability is written (eq. (12.26)):

$$P(\bar{\nu}_{\mu}) \to^{(\bar{\nu}_{\mu})} = 1 - \sin^{2}(2\theta_{12})\cos^{4}(\theta_{23})\sin^{2}\left(x\frac{\delta m_{21}^{2}}{4k}\right)$$

$$- \left[\sin^{2}(2\theta_{23})\cos^{2}(\theta_{13}) + \sin^{2}(2\theta_{13})\sin^{4}(\theta_{23})\right]\sin^{2}\left(x\frac{\delta m_{32}^{2}}{4k}\right)$$

$$- 16 J \sin^{2}(\theta_{23})\cos(\delta)\sin\left(x\frac{\delta m_{21}^{2}}{4k}\right)\sin\left(x\frac{\delta m_{32}^{2}}{4k}\right)\cos\left(x\frac{\delta m_{32}^{2}}{4k}\right),$$

$$(14.7)$$

and the oscillation probability is (see eq. (12.41):

$$P(\bar{\nu}_{\mu}) \to (\bar{\nu}_{e}) = \sin^{2}(2\theta_{13}) \sin^{2}(\theta_{23}) \sin^{2}\left(x\frac{\delta m_{32}^{2}}{4k}\right) + \sin^{2}(2\theta_{12}) \cos^{2}(\theta_{23}) \sin^{2}\left(x\frac{\delta m_{21}^{2}}{4k}\right)$$

$$+ 8J \sin\left(x\frac{\delta m_{21}^{2}}{4k}\right) \sin\left(x\frac{\delta m_{32}^{2}}{4k}\right) \left[\cos(\delta) \cos\left(x\frac{\delta m_{32}^{2}}{4k}\right) \pm \sin(\delta) \sin\left(x\frac{\delta m_{32}^{2}}{4k}\right)\right].$$
(14.8)

where the - sign is for neutrino and the + sign for antineutrinos.

<sup>&</sup>lt;sup>53</sup>H. de Kerret *et al.*, arXiv:1901.09445 [hep-ex].

<sup>&</sup>lt;sup>54</sup>T2K collaboration, K.Abe *et al.*, Phys. Rev. Lett. **107** (2011) 041801, arXiv:1106.2822 [hep-ex].

<sup>&</sup>lt;sup>55</sup>T2K collaboration, K.Abe et al., Phys. Rev. D 96 (2017) 092006, arXiv:1707.01048 [hep-ex].

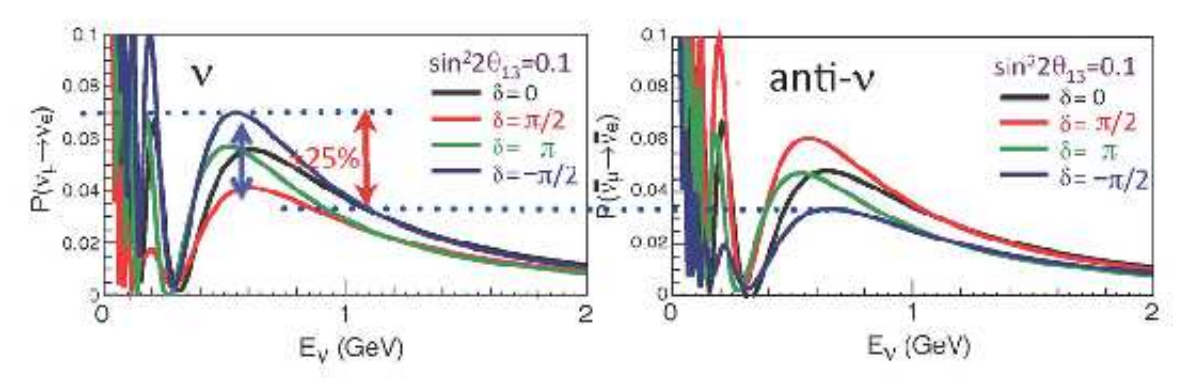


Figure 9: Comparison of the oscillation rate  $\overline{\nu}_e$  in a  $\overline{\nu}_\mu$  beam (right) with that of  $\nu_e$  in a  $\nu_\mu$  beam (left) for differente hypothesis on the CP violation parameter  $\delta$ . Note that  $\delta = -\pi/2$  in the figure corresponds to  $\delta = 3\pi/2$  in the text. From Y. Oyama, for T2K Collaboration, PoS PLANCK2015 (2015) 094, arXiv:1510.07200 [hep-ex].

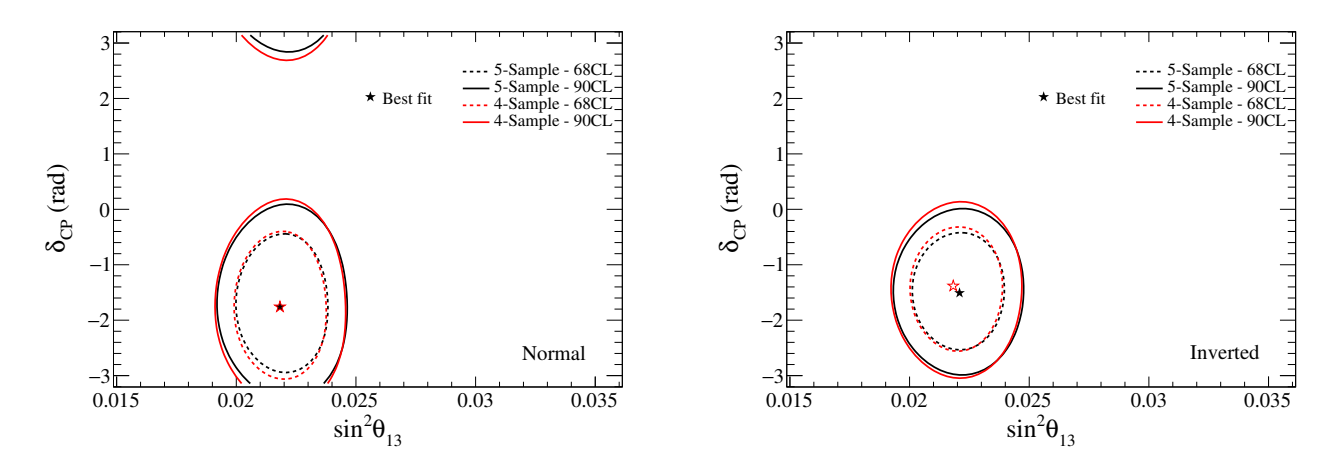


Figure 10: Joint fit of  $\sin^2(\theta_{13})$  and  $\delta$  to the data of appearance of  $\nu_e$  in a  $\nu_\mu$  beam and  $\overline{\nu}_e$  in a  $\overline{\nu}_\mu$  beam, for both mass hierarchy hypotheses:  $\Delta\chi^2$  contours using 5-sample data (black) or 4-sample data (red). Constraints from reactors data are included.  $\delta$  in the text is  $2\pi + \delta_{CP}$  in the figures. From T2K Collaboration, K. Abe et al., Phys. Rev. **D 96** (2017) 092006, arXiv:1707.01048 [hep-ex].

For the T2K configuration, the  $\sin\left(x\,\delta m_{21}^2/4k\right)$  term is very small ( $\approx 0.048$ ) compared to  $\sin\left(x\,\delta m_{32}^2/4k\right)$  which justifies the neglect of terms in  $\sin^2\left(x\,\delta m_{21}^2/4k\right)$  in the cofficient of J (see eqs. (12.38) and (12.40)). Since  $\sin^2(2\theta_{13}) \approx .084$  is small, we drop such terms in the coefficient of  $\sin^2\left(x\,\delta m_{21}^2/4k\right)$  but keep them in the coefficient of  $\sin^2\left(x\,\delta m_{32}^2/4k\right)$ . The survival probabilities are dominated by the  $\sin^2(2\theta_{23})\sin^2\left(x\,\delta m_{32}^2/4k\right)$  piece and lead to a good determination of  $\theta_{23}$  and  $\delta m_{32}^2$ . Based on data collected until 2016 the T2K collaboration quotes the values, at a 1  $\sigma$  confidence level:

$$\delta m_{32}^2 = (2.54 \pm 0.08) \, 10^{-3} \, \text{eV}^2, \quad \sin^2(\theta_{23}) = 0.55 \, ^{+0.05}_{-0.09}$$
 (14.9)

for normal mass ordering, and

$$\delta m_{32}^2 = (2.51 \pm 0.08) \, 10^{-3} \, \text{eV}^2, \quad \sin^2(\theta_{23}) = 0.55 \, ^{+\ 0.05}_{-\ 0.08}$$
 (14.10)

for inverted mass ordering. For this value of  $\delta m_{32}^2$  and for a peak energy of .6 GeV and the base line of 295 km one finds  $\cos\left(x\,\delta m_{32}^2/4k\right)\approx 0$  which means that the  $\cos(\delta)$  term has almost no contribution to the survival or oscillation probabilities. Since it is the only term which changes sign when going from normal to inverted hierarchy, T2K is not sensitive to the sign of  $\delta m_{32}^2 \approx \delta m_{31}^2$ . The  $\delta$  dependence of  $P(\nu_{\mu} \to \nu_e)$  is therefore almost entirely given by the  $\sin(\delta)$  piece which is

$$-8 J \sin\left(x\frac{\delta m_{21}^2}{4k}\right) \sin^2\left(x\frac{\delta m_{32}^2}{4k}\right) \sin(\delta)$$

$$\approx -\sin(2\theta_{12}) \sin(2\theta_{23}) \sin(2\theta_{13}) \cos(\theta_{13}) \sin\left(x\frac{\delta m_{21}^2}{4k}\right) \sin^2\left(x\frac{\delta m_{32}^2}{4k}\right) \sin(\delta)$$

$$\approx -0.013 \sin(\delta) \tag{14.11}$$

for the peak energy of 0.6 GeV. Furthermore the variation of  $P(\overline{\nu}_{\mu} \to \overline{\nu}_{e})$  as a function of  $\delta$  is opposite to that of  $P(\nu_{\mu} \to \nu_{e})$ . The amplitude of variation is about 0.026 when going from  $\delta = \pi/2$  to  $\delta = 3\pi/2$  as illustrated in fig. 9. From the oscillation data the collaboration quotes the following results, at a 1  $\sigma$  confidence level, taking into account the reactor constraints on  $\theta_{13}$ :

$$\delta = 4.56 \, {}^{+0.81}_{-0.85} \, (1.45 \, \pi_{-0.27 \, \pi}^{+0.26 \, \pi})$$
 for normal mass order,  
 $\delta = 4.83 \, {}^{+0.68}_{-0.73} \, (1.54 \, \pi_{-0.23 \, \pi}^{+0.22 \, \pi})$  for inverted mass order.

The correlation  $\delta - \sin(\theta_{13})$  is illustrated in fig. 10. The best fit value of the  $\mathcal{CP}$  violating angle is  $\delta \approx 3\pi/2$ , which means  $\cos(\delta) \approx 0$  and, consequently, it will be difficult to solve the hierarchy problem from any oscillation experiment in vacuum. In principle, since the neutrinos propagate through the Earth crust on a distance of about 300 km, matter effects should be taken into account when extracting the values of parameters. However, for a peak energy  $E_{\nu} = 0.6$  GeV and a density of electrons in the Earth crust around  $N_e = 8 \ 10^{23} \ \mathrm{cm}^{-3}$ , the relevant parameter  $\hat{A} = 2\sqrt{2}G_F N_e E_{\nu}/\delta m_{31}^2$  is very small,  $\hat{A} \approx 0.05$ , leading to negligible matter effects.

NO $\nu$ A is another long baseline accelerator experiment, optimised to study  $\nu_{\mu} \leftrightarrow \nu_{e}$  oscillations, which started publishing results recently<sup>56</sup>. It is a  $\nu_{\mu}$  disappearance  $\nu_{e}$  appearance experiment for both neutrinos and antineutrinos, with a beam of peak energy  $E_{\nu} \approx 2$  GeV from Fermilab with a far

 $<sup>^{56}</sup>$ NO $\nu$ A collaboration, P. Adamson, Phys. Rev. Lett. **118** (2017) 231801, arXiv:1703.03328 [hep-ex]; Jianming Bian, for the NO $\nu$ A collaboration, arXiv:1812.09585 [hep-ex].

detector 810 km away in Minnesota. With this choice of parameters, the value of  $\sin^2(x\delta m_{32}^2/E_{\nu})$  is near its maximum which maximizes the disappearance of  $\nu_{\mu}$  and the appearance of  $\nu_{e}$ . NO $\nu$ A has collected an equivalent of 8.85  $10^{20}$  protons on target for neutrinos and 6.9  $10^{20}$  for antineutrinos. It should be more sensitive to matter effects than T2K with a value of  $\hat{A} \approx .18$ . A preliminary analysis, for normal hierarchy (with  $\delta m_{31}^2 \approx \delta m_{32}^2$ ), yields  $\delta m_{32}^2 = 2.51^{+0.12}_{-0.08} \, 10^{-3} \, \text{eV}^2$  with a mixing angle,  $\sin^2(\theta_{23}) = .58 \pm .03$ .

OPERA is a  $\tau$  appearance experiment: it is the only detector designed to identify  $\tau$  leptons in a  $\nu_{\mu}$  beam on an event-by-event basis. The  $\nu_{\mu}$  source is the CNGS (CERN Neutrinos to Gran Sasso) beam directed at the Grand Sasso underground facility 730 km away. Compared to other accelerator experiments the  $\nu_{\mu}$  energy is very high,  $\langle E_{\nu_{\mu}} \rangle = 17$  GeV to overcome the  $\tau$  production threshold,  $E_{th} = 3.55$  GeV. The observed number of  $\tau$  leptons is written<sup>57</sup>

$$N_{\tau} = A \int_{E_{th}} \Phi_{\nu_{\mu}}(E) P(\nu_{\mu} \to \nu_{\tau}) \, \sigma_{\tau}^{CC}(E) \, \varepsilon(E) \, dE, \qquad (14.12)$$

where A is a normalisation constant taking account of the detector mass,  $\Phi_{\nu_{\mu}}(E)$  the neutrino flux,  $\sigma_{\tau}^{CC}(E)$  the charged-current  $\nu_{\tau}$  cross section and  $\varepsilon(E)$  the  $\nu_{\tau}$  detection efficiency. As for  $P(\nu_{\mu} \to \nu_{\tau})$  the oscillation rate given in eq. (12.33), it simplifies considerably since the  $\sin^2(\delta m_{12}^2 x/4k)$  term with  $\delta m_{12}^2 x/4k \approx 4.1 \, 10^{-3}$  gives a negligeable contribution,

$$P(\nu_{\mu} \to \nu_{\tau}) \approx \sin^2(2\theta_{23}) \sin^2(\delta m_{32}^2 x/4k)$$
 (14.13)

ignoring furthermore  $\sin^2(\theta_{13})$  pieces. For the OPERA configuration the number of observed  $\tau$  leptons is given<sup>58</sup>

$$N_{\tau} \approx A' \sin^2(2\theta_{23}) \left(\delta m_{32}^2 [\text{eV}^2] L[\text{km}]\right)^2 \int_{E_{th}} \Phi_{\nu_{\mu}}(E) \, \sigma_{\tau}^{CC}(E) \, \varepsilon(E) \frac{dE}{E^2}.$$
 (14.14)

In 2010 the first observation of a  $\tau$  lepton in a  $\nu_{\mu}$  beam<sup>59</sup> was made. According to the final results<sup>60</sup> 10  $\nu_{\tau}$  candidate events have been reported, for an expected no oscillation background of 2 events, which allows to claim for the discovery of  $\nu_{\mu} \to \nu_{\tau}$  oscillations with a significance level of 6.1  $\sigma$ . A value of  $\delta m_{32}^2 = 2.7_{-0.6}^{+0.7} \, 10^{-3} \, \text{eV}^2$  is obtained, consistent with the world average.

 $<sup>^{57}</sup>$  OPERA Collaboration, S. Dusini, AIP Conference Proc. **1666** (2015) 110003; doi: 10.1063/1.4915575.

<sup>&</sup>lt;sup>58</sup>In this expression the approximation  $\sin\left(L\,\delta m_{32}^2/4E\right) \approx 1.27\,\delta m_{32}^2[\text{eV}^2]\,L[\text{km}]/E[\text{GeV}]$  is justified.

<sup>&</sup>lt;sup>59</sup>OPERA Collaboration, N. Agafonova et al. Phys. Lett. B 691 (2010) 138, arXiv:1006.1623.

<sup>&</sup>lt;sup>60</sup>N. Agafonava *et al.* Phys. Rev. Lett. **120** (2018) 211801, arXiv:1804.04912 [hep-ex].

## 14.3 Atmospheric neutrinos: Super-Kamiokande; $\delta m_{32}^2$ , $\theta_{23}$ , $\delta$

In 1998, the collaboration provided the first experimental evidence of neutrino oscillations<sup>61</sup>. Super-Kamiokande is an underground detector of 50 kilotons of ultra-pure water located in Gigu prefecture in Japan. It records the  $\mu^{\pm}$  and  $e^{\pm}$  produced in  $\overline{\nu}$  and  $\nu$  induced reactions. In a first analysis it is difficult to tell  $\nu_{\mu}$  ( $\nu_{e}$ ) from  $\overline{\nu}_{\mu}$  ( $\overline{\nu}_{e}$ ) so that the results are given for  $\nu_{\mu} + \overline{\nu}_{\mu}$  and  $\nu_{e} + \overline{\nu}_{e}$  fluxes. One distinguishes the downward going flux (zenithal angle  $\theta_{z} \approx 0$ ) with the neutrinos interacting (primary vertex) in the detector after a path length of 1 to 30 km in the atmosphere, from the upward going flux (zenithal angle  $\theta_{z} \approx \pi$ ) where the neutrinos, after travelling up to 1.3 10<sup>4</sup> km through the Earth, are interacting in the rocks outside Super-K producing a muon energetic enough to enter the detector<sup>62</sup>. In a first approximation (e.g.  $x/k < 10^{3}$ ) one ignores the oscillation terms in  $\sin(\delta m_{21}^{2}x/4k)$  and take  $\delta m_{32}^{2} \approx \delta m_{31}^{2}$ . The relevant rates of oscillations (in vacuum) are obtained from secs. 12.3 and 12.4:

$$P(\nu_{e} \leftrightarrow \nu_{\mu}) \approx \sin^{2}(2\theta_{13}) \sin^{2}(\theta_{23}) \sin^{2}(\delta m_{31}^{2} x/4 k)$$

$$P(\nu_{e} \to \nu_{\tau}) \approx \sin^{2}(2\theta_{13}) \cos^{2}(\theta_{23}) \sin^{2}(\delta m_{31}^{2} x/4 k)$$

$$P(\nu_{\mu} \to \nu_{\tau}) \approx \sin^{2}(2\theta_{23}) \cos^{4}(\theta_{13}) \sin^{2}(\delta m_{31}^{2} x/4 k)$$

$$P(\nu_{e} \to \nu_{e}) \approx 1 - \sin^{2}(2\theta_{13}) \sin^{2}(\delta m_{31}^{2} x/4 k)$$

$$P(\nu_{\mu} \to \nu_{\mu}) \approx 1 - [\sin^{2}(2\theta_{23}) \cos^{2}(\theta_{13}) + \sin^{2}(2\theta_{13}) \sin^{4}(\theta_{23})] \sin^{2}\left(x \frac{\delta m_{31}^{2}}{4k}\right).$$
(14.15)

One checks easily that  $P(\nu_{\mu} \to \nu_{\mu}) = 1 - P(\nu_{\mu} \to \nu_{e}) - P(\nu_{\mu} \to \nu_{\tau})$ . We quote here very simplified formulae which are sufficient to understand the global features of the data but, in their analysis, the Super-K collaboration uses the full model including the  $\mathcal{CP}$  violating phase  $\delta$  as well as matter effects. From eqs. (14.15) it is expected that  $\nu_{\mu}$  will fluctuate dominantly in  $\nu_{\tau}$  ( $\sin^{2}(2\theta_{23}) \approx .99 \ vs$   $\sin^{2}(2\theta_{13}) \approx .1$ ) and the  $\nu_{\mu}$  disappearance will be less important for downward neutrinos since they do not have time to oscillate unlike those crossing the Earth. Because of the small value of  $\sin^{2}(2\theta_{13})$   $\nu_{e}$  oscillation is less effective.

The Super-K collaboration has given the most precise measurements of the atmospheric neutrino fluxes in a large energy range<sup>63</sup>:  $0.15 < E_{\nu} \, [{\rm GeV}] < 65$  for  $\nu_e + \overline{\nu}_e$  and  $0.25 < E_{\nu} \, [{\rm GeV}] < 2500$  for  $\nu_{\mu} + \overline{\nu}_{\mu}$  (see fig. 11 which also displays model predictions with and without oscillations). At high energies, the spectrum is dominated by  $\nu_{\mu} + \overline{\nu}_{\mu}$  and, for kinematical reasons, the  $\nu_{\tau}$  flux is negligible. As expected the  $\nu_e + \overline{\nu}_e$  flux is globally not sensitive to oscillations while the  $\nu_{\mu} + \overline{\nu}_{\mu}$  flux below 100

<sup>&</sup>lt;sup>61</sup>Super-Kamiokande Collaboration, Y. Fukuda et al. Phys. Rev. Lett. 81 (1998)1562, arXiv:hep-ex/9807003.

<sup>&</sup>lt;sup>62</sup>More precisely, the downward neutrinos have  $0 < \theta_z < \pi/2$  and the upward neutrinos have  $\pi/2 < \theta_z < \pi$ .

<sup>&</sup>lt;sup>63</sup>Super-Kamiokande collaboration, E. Richard et al., Phys. Rev. D94 (2016) 052001, arXiv:1510.08127 [hep-ex].

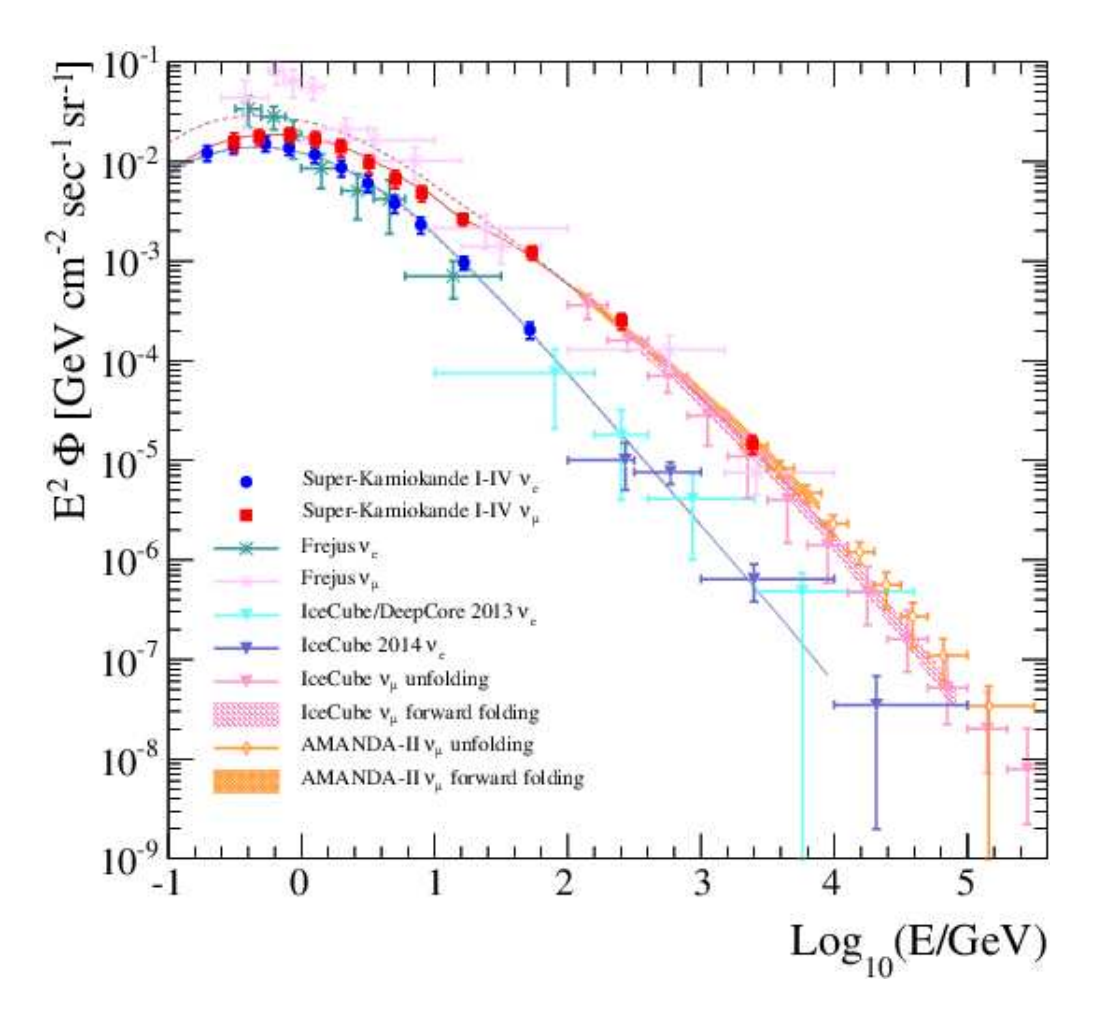


Figure 11: Energy spectra of  $\nu_e + \overline{\nu}_e$  and  $\nu_\mu + \overline{\nu}_\mu$  atmospheric neutrinos by the Super-K collaboration in comparison with other measurements. The solid (dashed) lines are model predictions with (without) oscillations. From Super-Kamiokande collaboration, E. Richard et al., Phys. Rev. **D94** (2016) 052001, arXiv:1510.08127 [hep-ex].

GeV is reduced. Above this energy the factor  $(x \, \delta m_{31}^2/4 \, k)$  is small and oscillations become irrelevant. Fig. 12 displays details of  $\nu$  oscillations in the Earth. Panel b) illustrates the survival pattern of an upward  $(\cos \theta_z = -1) \, 4 \, \text{GeV} \, \nu_\mu$  as a function of the distance travelled in the Earth. After crossing the Earth  $(x \approx 1.28 \, 10^4 \, \text{km})$  the neutrinos have undergone 3 cycles of oscillations i.e.  $(x \delta m_{31}^2/4k) \approx 3 \, \pi$ . Notice that, in the model illustrated in fig. 12-b, the oscillation strength is enhanced as the muon neutrino crosses the Earth indicating a modification of the mixing angles (see eqs. (13.49)). A naive estimate of the effect of matter is obtained by calculating the factor  $\hat{A}$ , eq. (13.46):

$$\hat{A} = \frac{2\sqrt{2}G_F N_e E_{\nu}}{\delta m_{31}^2} \approx .1 \left(\frac{E_{\nu}}{[GeV]}\right), \quad \text{for } N_e \approx 1.10^{24} \text{cm}^{-3}.$$

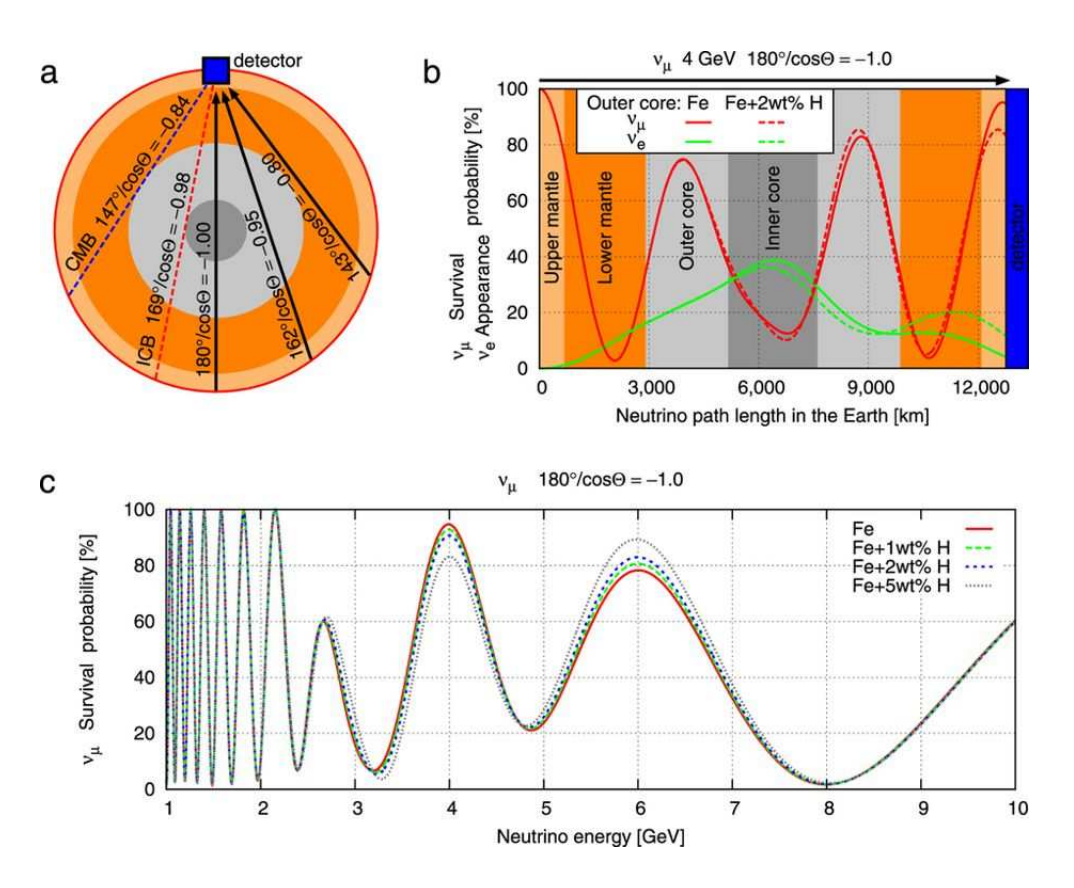


Figure 12: Neutrino oscillation patterns in the Earth. a) definition of the zenith angle  $\theta$ , denoted  $\theta_z$  in the text, and multilayer structure of the Earth; the average density of electrons in the core (grey areas) is  $N_e^{core} \approx 3.3\,10^{24}\,\mathrm{cm}^{-3}$ , and in the mantle (red area)  $N_e^{mantle} \approx 1.2\,10^{24}\,\mathrm{cm}^{-3}$ ; b) survival probability of an upward (cos  $\theta = -1$ ) E = 4 GeV muon neutrino crossing the Earth (red) and correlated appearance probability of an electron neutrino (green); c) survival probability of an upward going muon neutrino having crossed the Earth as a function of energy. From C. Rott, A. Taketa, D. Bose, Nature Scientific Reports: 15225, www.nature.com/articles/srep15225.

Panel c) illustrates, as a function of energy, the survival pattern of an upward muon neutrino exiting from the Earth: because of the 1/k dependence of the oscillating factor, oscillations are much more rapid at low energy. In data, an average over a large energy range is performed so that the oscillating factor  $\sin^2(x\delta m_{31}^2/4k)$  reduces to .5.

The distribution of events as a function of the zenith angle is given in fig. 13: for events labelled "Multi-GeV  $\mu$ -like" (middle panel) the increase in the number of events when  $\cos \theta_z$  decreases from 1 to 0 is due to the increase of the effective thickness of the atmosphere, then at  $\cos \theta_z = -1$  the oscillations reduce the  $\nu_{\mu} + \overline{\nu}_{\mu}$  flux by a factor 2 compared to the no oscillation expectation. Concerning  $\nu_e$ 's, the disappearance (left panels) is much less pronounced. One notices however that energetic upgoing

### SK-I+II+III+IV, 4581 Days

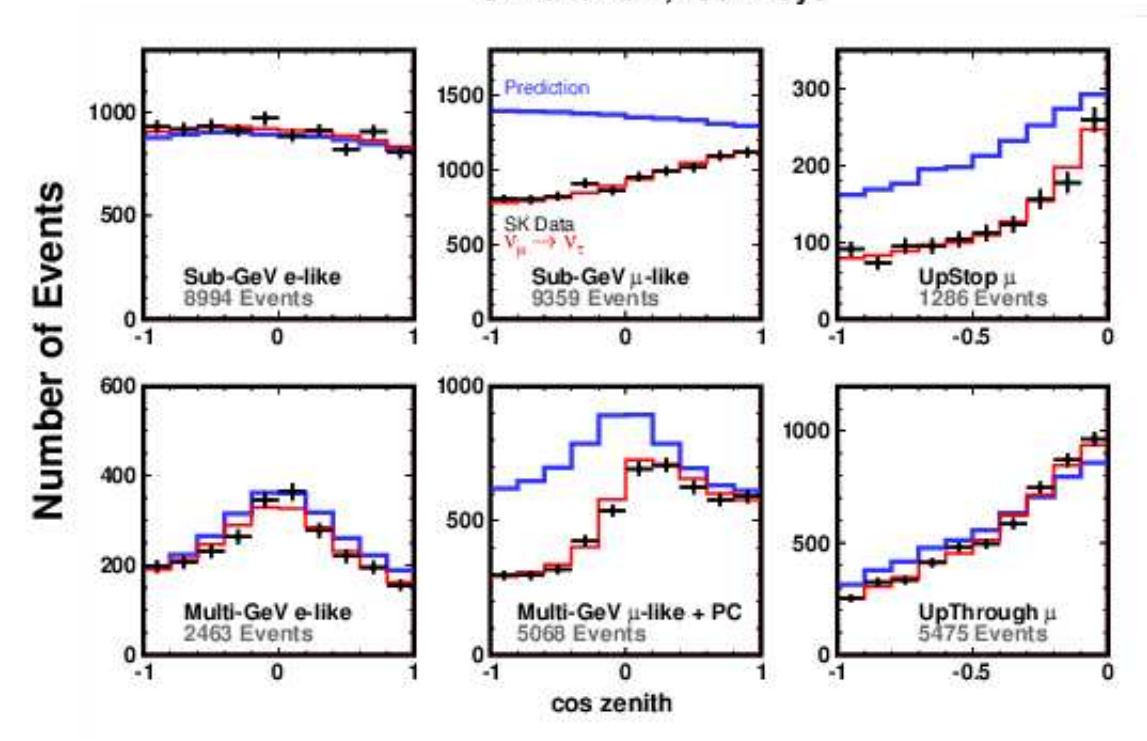


Figure 13: Superkamiokande zenithal oscillations: "Sub-GeV" refers to events with  $E_{vis} < 1.33$  GeV while "Multi-GeV refers to neutrinos with  $E_{vis} > 1.33$  GeV. The 4 left most panels have a reconstruted vertex in the SK detector while the 2 right most panels show the sample of upward-going muons produced by neutrinos in the rock surrounding the detector. The blue lines show the non-oscillated prediction and the red lines the oscillated ones. From R. Wendell for the Super-Kamiokande collaboration, arXiv:1412.5234 [hep-ex].

(anti)neutrinos are less suppressed than downgoing ( $\cos\theta_z\approx 1$ ) ones: at high energy the atmospheric  $\nu_\mu + \overline{\nu}_\mu$  flux is much larger than the  $\nu_e + \overline{\nu}_e$  flux and, furthermore, between 2 and 10 GeV the  $\nu_\mu + \overline{\nu}_\mu$  to  $\nu_e + \overline{\nu}_e$  resonant enhancement in the Earth is possible as discussed in sec. 13.3. The resonant enhancement is sensitive to the sign of  $\delta m_{31}^2$  and affects  $\nu_e$ 's for normal hierarchy and  $\overline{\nu}_e$ 's for inverted hierarchy. Separating neutrinos from antineutrinos would allow to determine the sign of  $\delta m_{31}^2$ . For this purpose the collaboration is constructing  $\nu_e$  and  $\overline{\nu}_e$  enriched samples.

In recent analyses of their data<sup>64</sup>, keeping the  $\delta$  dependence and matter effects as in eq. (13.56), for example, the Super-Kamiokande collaboration constrains several mixing parameters. The analyses are constrained, *i.e.* fixing  $\sin^2(\theta_{13})$ , or unconstrained. In the latter case the best fit for normal hierarchy gives  $\sin^2(\theta_{13}) = .008^{+0.025}_{-0.005}$  and:

$$\delta m_{31}^2 = (2.63^{+0.10}_{-0.21}) \, 10^{-3} \text{eV}^2, \qquad \sin^2(\theta_{23}) = 0.588^{+0.030}_{-0.062}, \qquad \delta = 3.84^{+2.00}_{-2.14} \, (1.22\pi^{+0.63\pi}_{-0.68\pi}), \, (14.16)$$

 $<sup>^{64}</sup>$ Super-Kamiokande collaboration, K. Abe et al., Phys.Rev. **D97** (2018) 072001, arXiv:1710.09126 [hep-ex].

while, fixing  $\sin^2(\theta_{13}) = 0.0210 \pm 0.0011$  (from the Daya Bay, RENO and Double-Chooz) the results are:

$$\delta m_{31}^2 = (2.53^{+0.22}_{-0.12}) \, 10^{-3} \mathrm{eV}^2, \qquad \sin^2(\theta_{23}) = 0.425^{+0.046}_{-0.037}, \qquad \delta = 3.14^{+2.67}_{-1.35} \, \, (\pi_{-0.43\pi}^{+0.85\pi}). \tag{14.17}$$

Very similar numbers are obtained for the inverted hierarchy hypothesis but the data indicate a weak preference for the normal mass hierarchy. One observes that, when constraining  $\theta_{13}$ , the  $\theta_{23}$  angle is in the first octant  $\theta_{23} < \pi/4$  but, for the other case,  $\theta_{23}$  is in the second octant  $\theta_{23} > \pi/4^{65}$ . This illustrates the strong correlations between parameters as shown by eqs. (14.15), as well as the difficulty to obtain a precise determination of the mixing angles.

The upper end of the  $\nu + \overline{\nu}$  spectra in fig. 11 do not play any role in the physics of oscillations but, as will be seen in sec. 14.5, they carry information on cosmic sources.

The parameters  $\delta m_{32}^2$  and  $\sin^2(\theta_{23})$  are often called atmospheric oscillation parameters.

## 14.4 Solar neutrinos: SNO; $\delta m_{12}^2$ , $\theta_{12}$

Since the mid sixties solar neutrinos presented a nagging problem: the measured flux<sup>66</sup> was two to three time smaller than the predicted one by the standard solar neutrino model<sup>67</sup>. Several explanations were proposed to account for this discrepancy<sup>68</sup> but now it has been shown that the correct explanation lies in the incoherent interactions of neutrinos with matter in the sun.

According to the standard solar neutrino model, the production modes of neutrinos are given in fig. 14. The most abondant one is

$$p + p \to D + e^+ + \nu_e \tag{14.18}$$

with .1 MeV  $< E_{\nu} <$  .4 MeV. The flux has been observed by the "Gallium" experiments, GALLEX<sup>69</sup>, SAGE<sup>70</sup> and GNO<sup>71</sup>, via the transition Gallium to Germanium  $\nu_e + ^{71}Ga \rightarrow e^- + ^{71}Ge$ , with a threshold of .233 MeV. They all show a deficit of  $\nu_e$ 's compared to the model, roughly  $\phi_{obs}(\nu_e)/\phi_{mod}(\nu_e) \approx .54$ . Later on, the SNO (Sudbury Neutrino Obervatory) collaboration measured the neutrino flux from the

<sup>65</sup> If  $\theta_{23} \approx \pi/4$  the interchange  $\theta_{23} \to \pi/2 - \theta_{23}$  leads to almost degenerate predictions for the observables, see eqs. (14.15).

<sup>&</sup>lt;sup>66</sup>Homestake experiment, R. Davis et al., Phys. Rev. Lett. **12** (1964) 302.

<sup>&</sup>lt;sup>67</sup>J.N. Bahcall, et al., Phys. Rev. Lett. 17 (1966) 398; J.N. Bahcall, A.M. Serenelli, S. Basu, Astrophys.J. 621 (2005) L85.

 $<sup>^{68}</sup>$ Bruno Pontecorvo sugested in 1977 neutrino oscillations as the most reasonable explanation for the observed  $\nu_e$  deficit, Dubna Report E10545, 1977; S.M. Bilenky, B. Pontecorvo, Comments Nuc. Part. Phys. 7 (1977) 149.

<sup>&</sup>lt;sup>69</sup>GALLEX Collaboration, W. Hampel et al., Phys. Lett. **B447** (1999) 127.

<sup>&</sup>lt;sup>70</sup>SAGE Collaboration, J.N. Abdurashitov et al., Phys. Rev. C80 (2009) 015807.

<sup>&</sup>lt;sup>71</sup>GNO Collaboration, M. Altmann *et al.*, Phys. Lett. **B616** (2005) 174; GALLEX + GNO, F. Kaether *et al.*, Phys. Lett. **B685** (2010) 47.

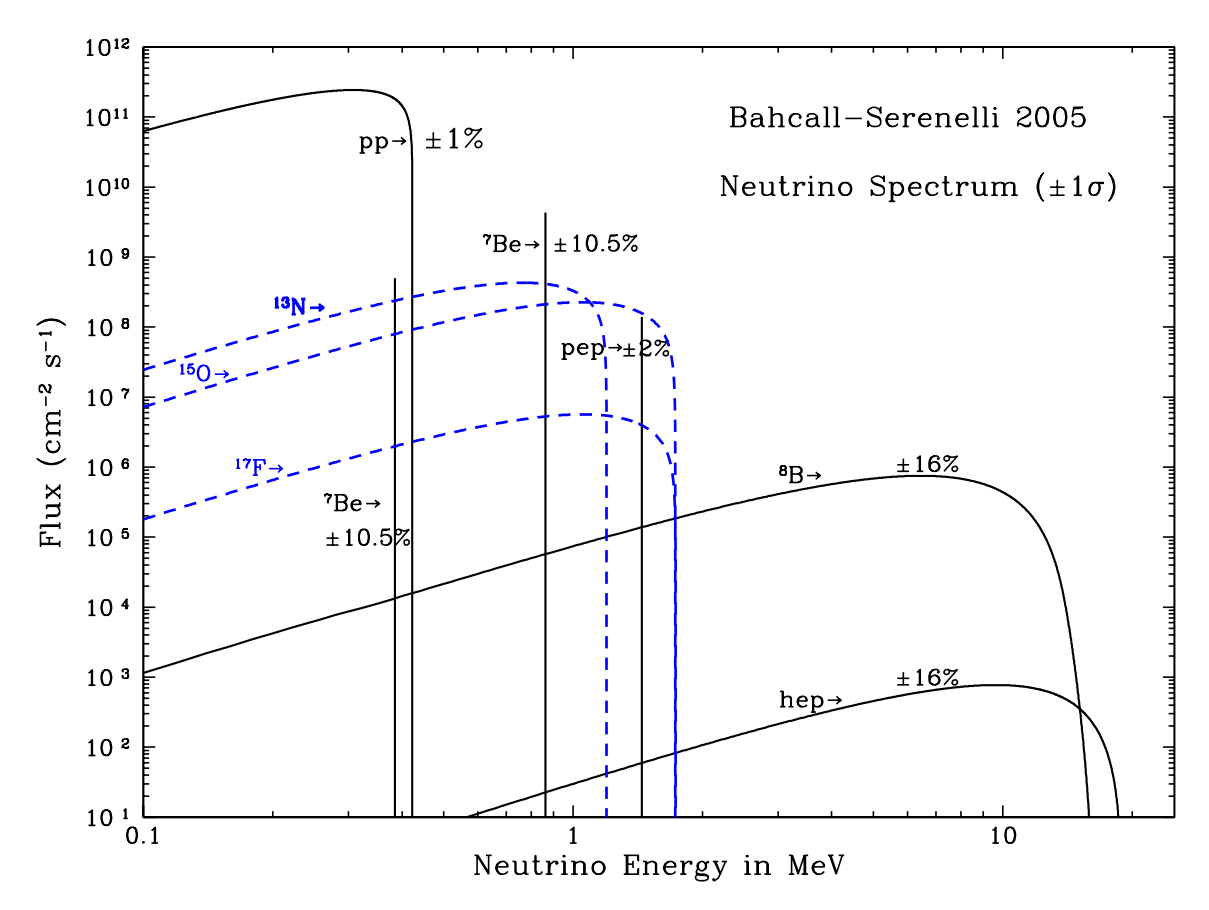


Figure 14: The solar neutrino spectrum from the sun (from J.N. Bahcall, A.M. Serenelli, S. Basu, Astrophys. J. 621 (2005) L85.

 $^8B$  decay into an excited beryllium state:

$$^{8}B \rightarrow ^{8}Be^{*} + e^{+} + \nu_{e}.$$
 (14.19)

It is essentially the only  $\nu_e$  source in the energy range 1.5 MeV  $< E_{\nu_e} <$  15. MeV but the solar  $\nu_e$ 's can convert to  $\nu_{\mu}$ 's and  $\nu_{\tau}$ 's on their way to the detector. The SNO collaboration<sup>72</sup> in Canada conducted an elaborate study of <sup>8</sup>B solar neutrinos. SNO is a detector using 1000 tons of ultra-pure heavy water  $(D_2O)$  surrounded by an ultra-pure water  $(H_2O)$  shield. Three types of reactions are studied

$$\nu_e + D \to p + p + e^-, \quad \text{via charged current (CC)}$$

$$\nu_x + D \to p + n + \nu_x, \quad \text{via neutral current (NC)}$$

$$\nu_x + e^- \to \nu_x + e^-, \quad \text{elastic scattering (ES)}, \quad (14.20)$$

<sup>&</sup>lt;sup>72</sup>SNO collaboration, B. Aharmim *et al.*, Phys. Rev. **C88** (2013) 025501, arXiv:1109.0763 [nucl-ex].

where  $\nu_x$  stands for  $\nu_e$ ,  $\nu_\mu$  or  $\nu_\tau$ . The Cherenkov light emitted by the electron in the final state is used to detect the first and third reactions and the second one is seen via the emission of a photon of 6.25 MeV emitted in the capture of the neutron on deuterium. The first reaction (CC), mediated by a W boson exchange, is only sensitive to electron neutrino while the second one (NC), mediated by Z boson exchange, receives an equal contribution from all three flavours

$$\sigma^{NC}(\nu_e) = \sigma^{NC}(\nu_\mu) = \sigma^{NC}(\nu_\tau) \tag{14.21}$$

For the third one,  $\nu_e$  has a higher cross section since it can go both by charged or neutral current as shown in fig. 15, and one has with a good approximation

$$\sigma^{ES}(\nu_{\mu}) = \sigma^{ES}(\nu_{\tau}) \approx 0.156 \ \sigma^{ES}(\nu_{e}) \tag{14.22}$$

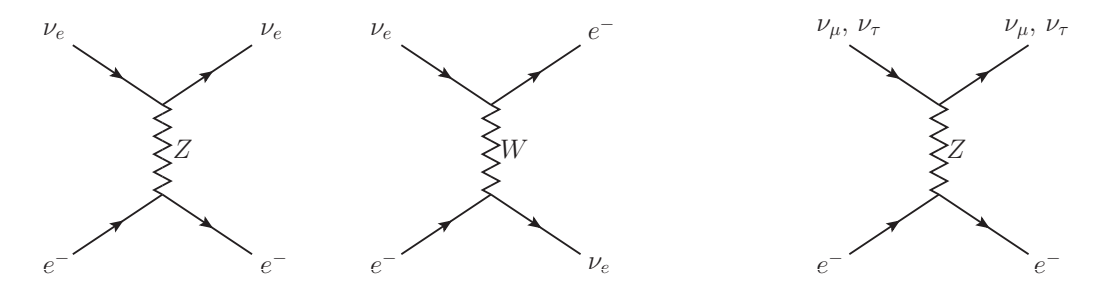


Figure 15: Feynman diagrams for the elastic diffusion of a neutrino on an electron: on the left for  $\nu_e$ , on the right for  $\nu_{\mu}$  or  $\nu_{\tau}$ .

The collaboration measures the flux of neutrinos in the various channels and finds (in units of  $10^6 \, \mathrm{cm}^{-2} \, \mathrm{s}^{-1}$ )

$$\phi^{CC} = \phi(\nu_e) = 1.76^{+0.06}_{-0.05} (\text{stat.})^{+0.09}_{-0.09} (\text{syst.})$$

$$\phi^{ES} = \phi(\nu_e) + 0.156 (\phi(\nu_\mu) + \phi(\nu_\tau)) = 2.39^{+0.24}_{-0.23} (\text{stat.})^{+0.12}_{-0.12} (\text{syst.})$$

$$\phi^{NC} = \phi(\nu_e) + \phi(\nu_\mu) + \phi(\nu_\tau) = 5.09^{+0.44}_{-0.43} (\text{stat.})^{+0.46}_{-0.43} (\text{syst.})$$
(14.23)

The result of  $\phi^{NC}$  is in very good agreement with the Standard Solar Neutrino Model<sup>73</sup>. From these results the collaboration derives (in the same units)

$$\phi(\nu_{\mu}) + \phi(\nu_{\tau}) = 3.41^{+0.45}_{-0.45} (\text{stat.})^{+0.48}_{-0.45} (\text{syst.}), \tag{14.24}$$

<sup>&</sup>lt;sup>73</sup>A.S. Brun, S. Turck-Chièze, J.P. Zahn, Astrophys. J. **525** (2001) 1032; J.N. Bahcall, M.H. Pinsonneault, S. Basu, Astrophys. J. **555** (2001) 990.

which is clear evidence for the disappearance of solar  $\nu_e$ 's. In later stages, the SNO collaboration improved the detection efficiency of neutrons by adding an array of  ${}^3He$  proportional counters in the  $D_2O$  volume and they obtain the most precise estimate of active neutrino flux (in units of  $10^6$  cm<sup>-2</sup> s<sup>-1</sup>)

$$\begin{array}{lcl} \phi^{NC} & = & 5.25 \, {}^{+\, 0.16}_{-\, 0.16} \, ({\rm stat.}) {}^{+\, 0.11}_{-\, 0.13} \, ({\rm syst.}) \\ \frac{\phi(\nu_e)}{\phi^{NC}} & = & .317 \pm 0.016 \, ({\rm stat.}) \pm 0.009 \, ({\rm syst.}), \quad {\rm at} \ E_{\nu} = 10 \ {\rm MeV}, \ {\rm independent \ on} \ E_{\nu}. \ (14.25) \end{array}$$

Because SNO observes  $\nu_e$  and  $\nu_{\mu} + \nu_{\tau}$  only, neither the mixing angle  $\theta_{23}$  nor the  $\mathcal{CP}$  violating phase play a role (see eqs. (12.25), (12.29), (12.32)). Furthermore, given the distance involved, 1.5  $10^9$  km, the argument of the oscillating factors are so large that the corresponding  $\sin^2$  terms reduce to 1/2. In vacuum, the  $\nu_e$  survival rate is then

$$P(\nu_e \to \nu_e) = 1 - \frac{1}{2}\sin^2(2\theta_{12})\cos^4(\theta_{13}) - \frac{1}{2}\sin^2(2\theta_{13})$$
$$= \sin^4(\theta_{13}) + (1 - \frac{1}{2}\sin^2(2\theta_{12}))\cos^4(\theta_{13}) \approx 1 - \frac{1}{2}\sin^2(2\theta_{12}), \qquad (14.26)$$

where the last approximate equality is a consequence of the smallness of  $\theta_{13}$ . It is then justified to use a two neutrino model. Assuming the validity of the oscillation model in vacuum to explain the SNO data, one would obtain

$$\frac{\phi(\nu_e)}{\phi^{NC}} \approx 1 - \frac{1}{2}\sin^2(2\theta_{12}) \approx 0.56,$$
 (14.27)

in contradiction with the SNO result of 0.317. The obvious conclusion is that neutrinos interact with matter in the sun.

#### • Neutrinos in the sun

The electron density in the sun is parameterised as<sup>74</sup>

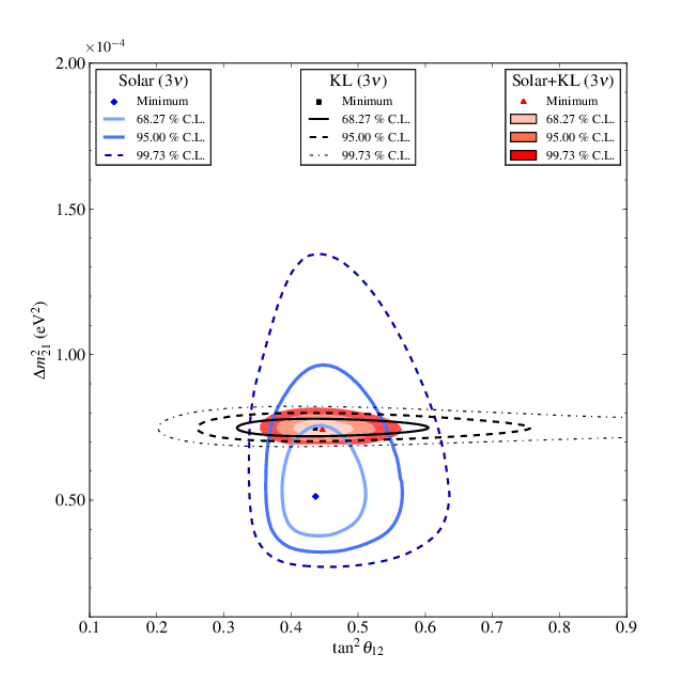
$$N_e(x) = N_e(x_0) \exp\left(\frac{x - x_0}{r_0}\right)$$
 (14.28)

with  $N_e(0) \approx 6$ .  $10^{25}$  and  $r_0 \approx .1 R_{\odot} \approx .7 10^5$  km (valid for  $x_0 \gtrsim .05 R_{\odot}$ ). If one uses for  $\delta m^2$  and  $\theta$  the values  $\delta m_{21}^2$  and  $\theta_{12}$  given by eq.(12.22) the adiabaticity condition eq. (13.31) will be satisfied if

$$\frac{1}{\hat{A}} \frac{r_0 \delta m_{12}^2}{2E_\nu} \sin^2(2\theta_{12}) \approx 2.7 \ 10^4 \left(\frac{E_\nu}{\text{MeV}}\right)^{-2} \gg 1,\tag{14.29}$$

where  $\hat{A}$  is taken from eq. (13.15). The inequality is satisfied for the SNO range of 5. MeV  $< E_{\nu} < 15$ . Mev. Besides  $\hat{A}$  remaining large (see secs. 13.3 and 13.4) one is justified to assume that the

<sup>&</sup>lt;sup>74</sup>J.N. Bahcall, Neutrino Astrophysics, Cambridge University Press, 1989.



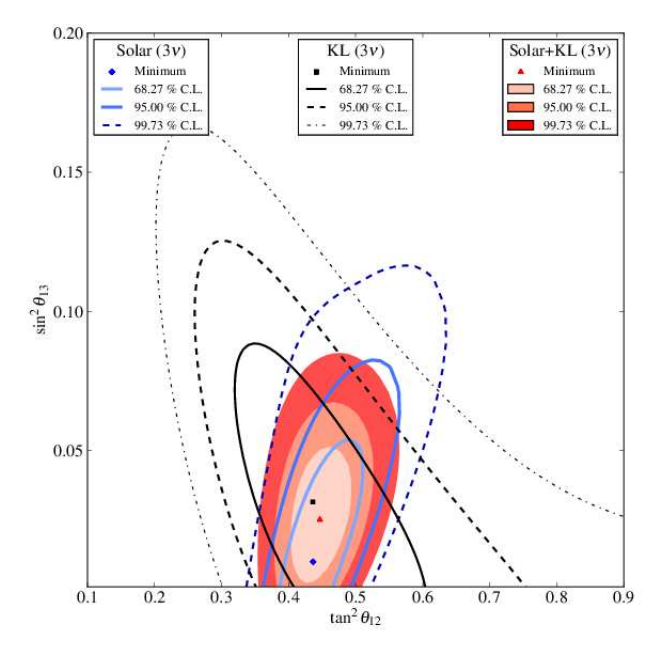


Figure 16: Three flavour neutrino oscillation analysis: the blue lines are obtained using all solar neutrino experiments, the black ones are from KamLAND data and the colored potatoes are from a joint analysis. (From SNO collaboration, B. Aharmim et al., Phys. Rev. C88 (2013) 025501, arXiv:1109.0763 [nucl-ex].)

neutrino is produced as the heaviest mass eigenstate and will emerge from the sun in a  $|\nu_2\rangle$  state with a probability  $P(\nu_e \to \nu_e; x_0, R) = \sin^2(\theta_{12})$  as in eq. (13.36). Being a pure eigenstate of the vacuum it will propagate without oscillation to Earth and will give

$$\frac{\phi(\nu_e)}{\phi^{NC}} = \sin^2(\theta_{12}) \approx .325,$$
 (14.30)

in good agreement, within errors, with the experimental result of eq. (14.25). Based on their flux measurements the SNO collaboration performs a two flavour and a three flavour neutrino oscillation analysis. However SNO data alone are not sufficient to give tight constraints on the parameters  $\delta m_{12}^2$ ,  $\theta_{12}$  so an analysis is performed using also other solar data as well as KamLAND reactor data. Fig. 16 shows the constraints provided by SNO alone as well as various combinations of data. The best fit to the joint data, in the three flavour analysis, yields:

$$\delta m_{21}^2 = (7.46^{+0.20}_{-0.19}) \, 10^{-5} \text{eV}^2, \qquad \tan^2 \theta_{12} = 0.443^{+0.030}_{-0.025}, \qquad \sin^2 \theta_{13} = (2.49^{+0.20}_{-0.32}) \, 10^{-2}, \qquad (14.31)^{-1} \, \text{eV}^2$$

in very good agreement with eq. (12.22). Coming back to the case of low energy neutrinos from

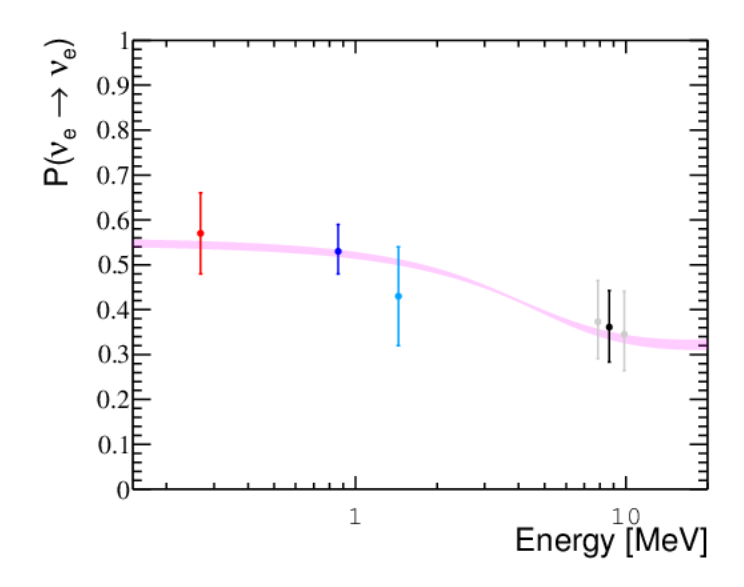


Figure 17: Summary of solar  $\nu_e$  survival probabilities as a function of the average neutrino energy.  $\nu_e$ 's produced in the pp reactions eq. (14.18): red point; in the  ${}^7\!Be + e^- \rightarrow {}^7\!Li + \nu_e$  channel: blue point; in the  $p + e^- + p \rightarrow D + \nu_e$  channel: light blue point; in the  ${}^8\!B$  channel eq. (14.19): black and grey points. The band is the theoretical prediction from the standard solar model with the MSW effect. The figure is from Borexino Collaboration, M. Agostini et al., arXiv:1709.00756 [hep-ex].

reaction eq. (14.18), the adiabatic condition is still verified but, in this case, the resonance condition cannot be satisfied since  $\hat{A} < \cos(2\theta_{12})$ , or equivalently  $N_e(x_0) < N_{\rm Res}$ , and interaction with matter becomes weaker. One expects from eq. (13.35) to have a larger ratio for  $\phi(\nu_e)/\phi^{NC}$  as is found by the collaborations GALLEX, GNO, SAGE and Borexino. In fact, for  $E_{\nu} \approx .2$  MeV, one finds  $N_e/N_{\rm Res} \approx .1$  from eq. (13.23) and, with a good approximation, the  $\nu_e$ 's should propagate as in vacuum with the result  $P(\nu_e \to \nu_e) = .56$  as in eq. (14.27) (see fig. 17).

The parameters  $\delta m_{21}^2$  and  $\theta_{12}$  are sometimes referred to as solar oscillation parameters and indexed with the symbol  $\odot$ .

### 14.5 Ultra-high energy or cosmic neutrinos

It is expected that, in the multi-TeV energy range and above, neutrinos from astrophysical or cosmic origin, will dominate over the atmospheric neutrinos. They can be produced in violent phenomena such as those occurring in Active Galactic Nuclei (AGN) or in collisions of ultra-high energy (UHE) cosmic rays on nucleons or photons, in particular photons from the cosmic microwave background (CMB). Neutrinos produced in a supernova event or in the merging of stars or black holes are expected to have energies in the MeV/GeV range. Unlike other cosmic messengers such as cosmic rays or photons the

universe is transparent to neutrinos<sup>75</sup>. Cosmic rays (protons, nuclei) are deflected by extra-galactic and galactic fields so that it is not possible to identify the source which produced them. They also loose energy when scattering on CMB photons, gaz and dust. Concerning photons, if their energy is high enough, they are absorbed on their way to Earth by  $e^+e^-$  pair production on CMB to UV

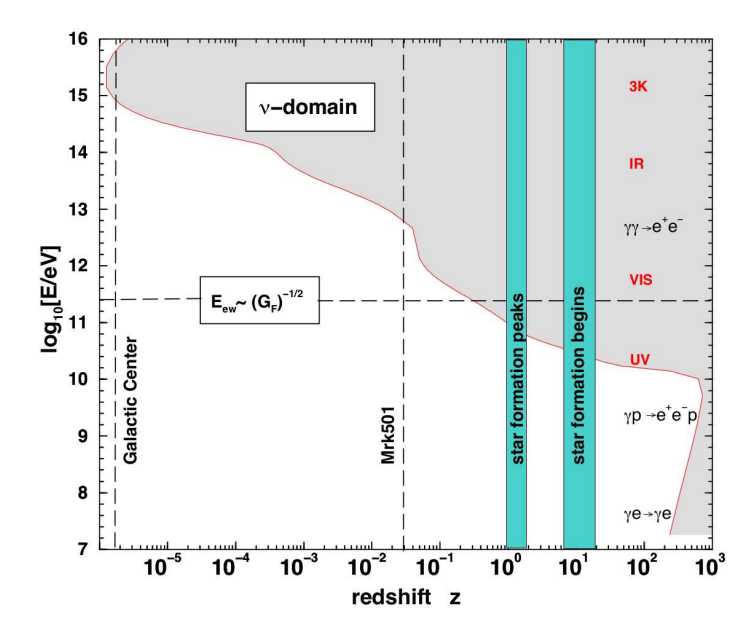


Figure 18: The photon horizon. Photons emittedinthegreymain do not reach the Earth because of annihilation  $e^+e^$ intoA redshift z = 1 corresponds to a distance of 14 Gly from the Earth. From J.G. Learned, K. Mannheim, Annual Rev. Nuc. Part. Sci. 50 (2000) 679.

background photons via  $\gamma_{HE} + \gamma_{bkgrd} \rightarrow e^+ + e^-$ . The threshold for such a process is obtained by solving the constraint  $(p_{\gamma_{HE}} + p_{\gamma_{bkgrd}})^2 > 4 \, m_e^2$ . Because of their high density ( $\sim 400 \, \mathrm{cm}^{-3}$ ) the CMB photons ( $E_{\gamma_{CMB}} \approx .23 \, \mathrm{meV}$ ) are particularly efficient in this respect cutting the high energy photon flux above  $10^{15} \, \mathrm{eV}$ : even those emitted nearby in the galactic center do not reach the Earth, as seen in Fig. 18. This figure illustrates the depth of the photon horizon as a function of the photon energy: for example a  $10^{12} \, \mathrm{eV}$  photon emitted by an object with a redshift z = .1 (*i.e.* roughly 1 Gly away) is absorbed before reaching the Earth. On the contrary, neutrinos are expected to travel undisturbed once they are emitted.

However the flux of UHE neutrinos is very low and to observe them requires huge detectors such as the km<sup>3</sup> IceCube detector<sup>76</sup> at the South Pole, the projected KM3NET<sup>77</sup> with a volume of 5 km<sup>3</sup> in the Mediterranean Sea which builds up on the ANTARES telescope<sup>78</sup> or the Giga Volume Detector<sup>79</sup> (GVD) which is an upgrade of the Lake Baikal experiment. As neutrino cross sections increase with

<sup>75</sup> The "Glashow resonance", i.e. the reaction  $\overline{\nu}_e + e^- \to W^- \to X$  should affect the  $\overline{\nu}_e$  flux above  $E_{\overline{\nu}_e} > 6.3 \, 10^{15}$  eV.

<sup>&</sup>lt;sup>76</sup>IceCube collaboration, Science **342** (2013) no. 6161.

<sup>&</sup>lt;sup>77</sup>KM3NET Collaboration, Maarten De Jong, PoS NEUTEL2015 (2015) 055

<sup>&</sup>lt;sup>78</sup>ANTARES Collaboration, Maurizio Spurio, PoS NEUTEL2015 (2015) 054.

<sup>&</sup>lt;sup>79</sup>BAIKAL-GVD Collaboration, A.D. Avrorin et al. (2015), DOI: 10.1142/9789814663618 0019.

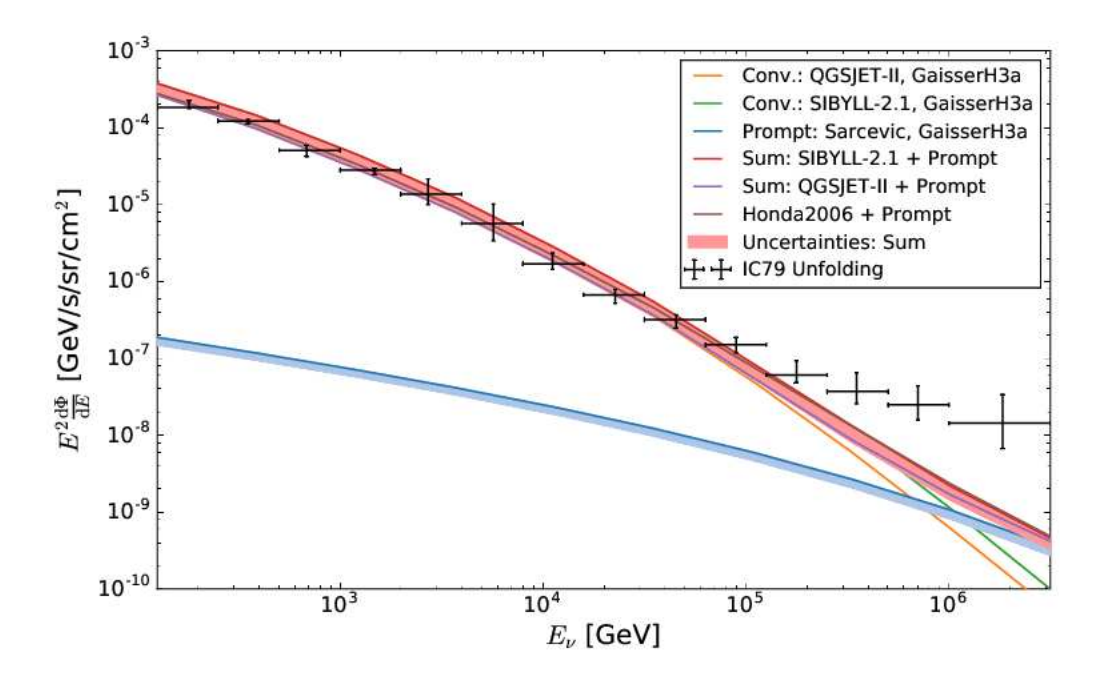


Figure 19: The high energy  $\nu_{\mu} + \overline{\nu}_{\mu}$  flux in IceCube, [arXiv:1705.07780].

energy the Earth will become opaque to neutrinos for  $E_{\nu} > 100$  TeV. The UHE neutrinos will then be searched for in the downward neutrino fluxes, but, in that case, the cosmic ray shower background will be enormous and must be vetoed.

IceCube recently extended the measurement of the  $\nu_{\mu} + \overline{\nu}_{\mu}$  flux above the domain shown in Fig. 11, up to more than 2 PeV<sup>80</sup>. The results are displayed in Fig. 19 where a hardening of the spectrum is observed above 100 TeV. Using a parameterisation of the cosmic ray flux and models of interactions of cosmic rays with the atmosphere they estimate the flux of atmospheric neutrinos: model and observation are in very good agreement up to around 100 TeV, energy above which the atmospheric neutrino flux falls below the data. The excess is interpreted as the flux of "astrophysical neutrinos" *i.e.* neutrinos directly emitted by sources such as AGN or produced in collisions of cosmic rays with dust, gaz or CMB photons.

On 22 September 2017 a high-energy neutrino-induced muon track event was detected by IceCube: the muon energy loss was estimated at  $23.7 \pm 2.8$  TeV corresponding to a probable parent neutrino energy of 290 TeV (event labelled IceCube-170922A)<sup>81</sup>. Furthermore the reconstructed neutrino direction appeared to be pointing at the known blazar TXS 0506+56 (redshift z=.3365). An automatic alert was activitated and led to the subsequent observation of very high energy gamma rays by the

<sup>&</sup>lt;sup>80</sup>IceCube collaboration, M.G. Aarsten et. al., EPJ **C77** (2017) 692, [arXiv:1705.07780].

<sup>&</sup>lt;sup>81</sup>IceCube collaboration, M.G. Aartsen et. al. Science **361** (2018) 347, [arXiv:1807.08794].

Fermi-LAT satellite and the Magic telescope by this blazar in a flaring state. Radio, optical, and X-ray observations were carried out and pointed to an increase of radio emission and variability in months before the alert and of X-ray emission a week after<sup>82</sup>.

This event is interesting as it is, at present, the only example of an identified neutrino emission from a blazar.

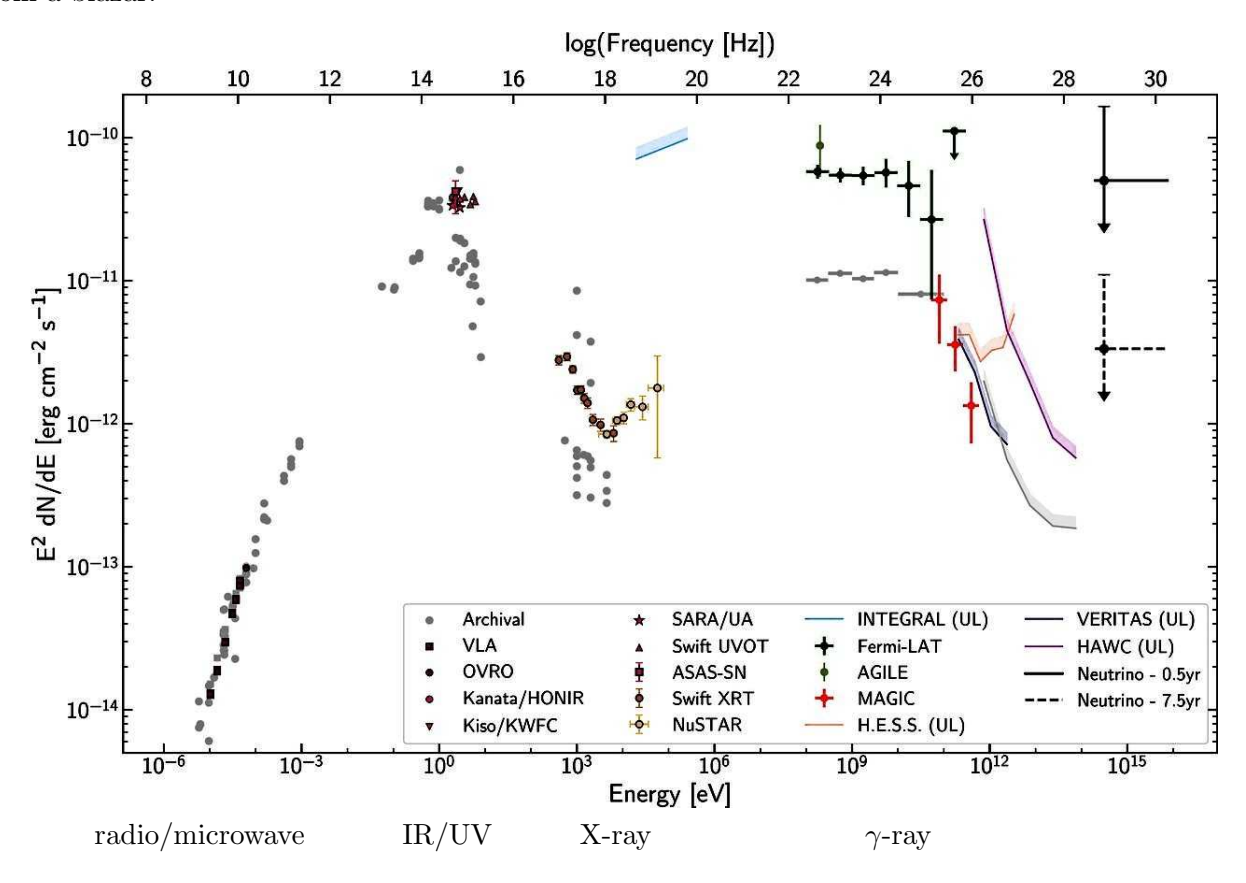


Figure 20: Spectral energy density of blazar TXS 0506+056 in a multi-messenger, multi-wave length analysis<sup>82</sup>. The rightmost two points are representative of  $\nu_{\mu} + \overline{\nu}_{\mu}$  flux upper limits that produce on average one detection like IceCube-170922A over a period of 0.5 year (solid black line) or 7.5 years (dashed black line) assuming a spectrum of  $dN/dE \propto E^{-2}$  at the most probable neutrino energy (311 TeV).

#### • Example of multi-messenger constraints on astrophysical $\nu$ emission

Fig. 20 shows the spectral energy density (SED) of TXS 0506+056 from radio to  $\gamma$ -ray energies as well as the upper limit of the neutrino contribution<sup>83</sup>. The characteristic two-peak structure of AGN

<sup>&</sup>lt;sup>82</sup>Science **361** (2018) no.6398, eaat1378,[arXiv:1807.08816].

<sup>&</sup>lt;sup>83</sup>For a review on multi-messenger studies of blazars see M. Böttcher, [arXiv:1901.04178].

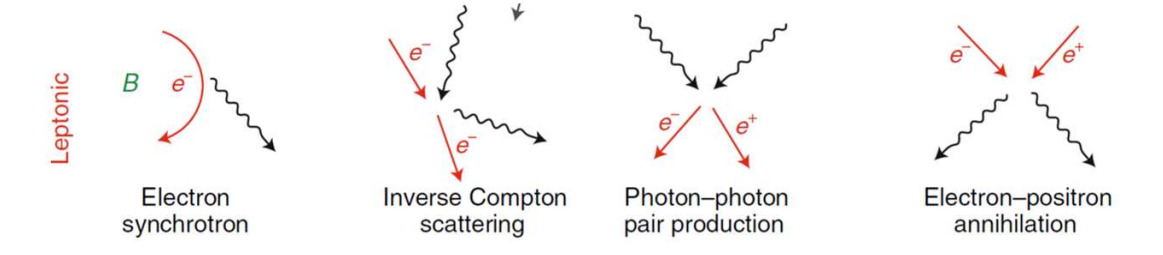


Figure 21: The dominant reactions in the leptonic model of AGN

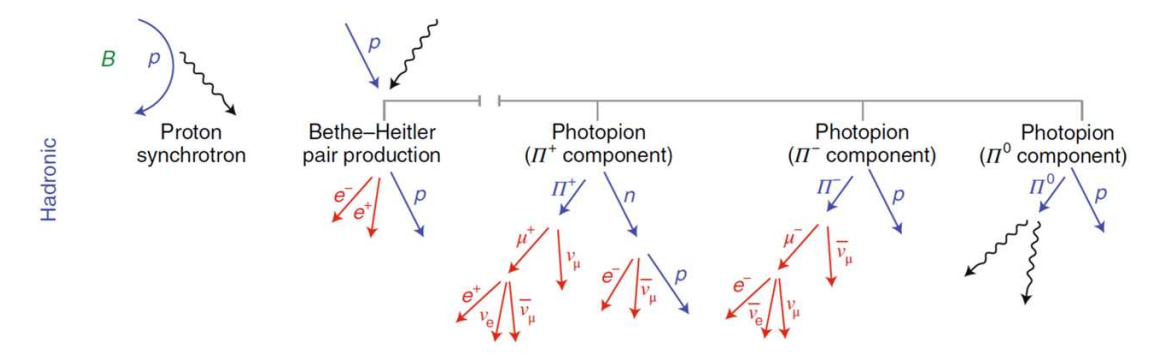


Figure 22: The dominant reactions in the hadronic model of AGN.

spectra is clearly visible<sup>84</sup>. The first peak is due to bremsstrahlung emission by relativistic electrons in the AGN jet but different models are used to explain the second peak. In leptonic models, Fig. 21, it is due to scattering of low energy bremsstrahlung photons on electrons producing them (synchrotron-self-Compton) or, more generally, to inverse Compton scattering; in this class of models protons in the jet are not accelerated to high enough energy to contribute to radiative energy even though they carry most of the kinetic energy of the jet. In hadronic models, Fig. 22, on the contrary, protons reach energies high enough to initiate photoproduction reactions on bremsstrahlung photons and produce pions. In more details one has the photoproduction of  $\pi^0$  via

$$\gamma + p \rightarrow \pi^0 + p$$
 followed by  $\pi^0 \rightarrow \gamma + \gamma$ 

and also production of  $\pi^{\pm}$ , e.g.

$$\gamma + p \to \pi^+ n, \qquad \gamma + p \to \pi^+ + \pi^- + \pi^0 + p$$
$$\pi^{\pm} \to \mu^{\pm} + \nu_{\mu}, \qquad \mu^{\pm} \to e^{\pm} + \nu + \overline{\nu}$$

Hadronic models then imply, from charged pion decays, the production of  $\nu'_e s$  and  $\nu'_\mu s$  carrying on the average 5% of the energy of the initiating proton. Knowing the energy of the neutrino detected on

<sup>&</sup>lt;sup>84</sup>An AGN consists typically in a supermassive rotating black hole in the center ( $10^6 M_{\odot}$  to  $10^{10} M_{\odot}$ ), an accretion disk, clouds of ionized gaz, a dust ring, two jets extending on 10's of parsecs and lobes extending on 100's of parsecs.

Earth it is then possible to estimate, after taking account of the relevant boost factor, the energy of the proton in the frame of the emission zone. An important feature is that hadronic models predict also the emission, from neutral pion decays, of ultra energetic photons in the same energy range as that of the neutrinos, namely hundreds of TeV. If these photons escape from the emission zone they are not seen on Earth because of  $e^+e^-$  pair production which would cut-off their flux (see the "photon horizon" cut-off on Fig. 18). Most of the ultra-high energy photons however are expected to be absorbed by  $e^+e^-$  pair creation in the emission zone and the  $e^{\pm'}s$  radiate, create electromagnetic cascades ending in the UV, X-ray or soft gamma regimes. In conclusion, in this model, the rate of emission of neutrinos is strongly constrained by the spectral energy density in the UV and X-ray range, but no very high energy photons are expected to be seen in association with  $\nu's$  observations. A model of SED spectra of TXS 0506+056 is shown in Fig. 23: it is seen that the hadronic component

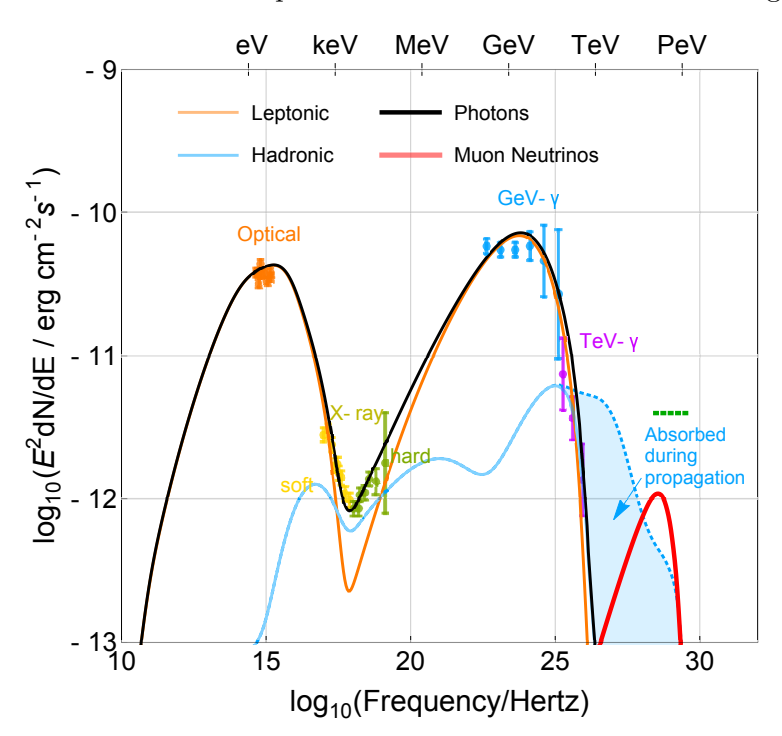


Figure 23: Spectral energy density of blazar TXS 0506+056 in the model of Shan Gao, A. Fedynitch, W. Winter, M. Pohl, Nat. Astron. 3 (2019) 88, [arXiv:1807.04275]. The red curve indicates the neutrino contribution assuming one  $\nu_{\mu}$  observation in 180 days. The emission of GeV  $\gamma$  rays is dominated by leptonic processes. The blue area shows the domain of absorbtion, by  $e^+e^-$  pair creation, of UHE photons on their way to Earth.

gives a major contribution to the spectral energy density in the X-ray range.

The above discussion illustrates how a multi-messenger analysis can constrain models and thereby help understand the physics of astrophysical objects.<sup>85</sup>

Coming back to neutrinos IceCube can, to some extent, determine the neutrino flavor. Using this

<sup>&</sup>lt;sup>85</sup>No neutrinos have been observed in correlation with the detection of gravitational waves emitted in the merging of black holes or neutron stars: ANTARES, IceCube and the Pierre Auger Observatory, Astrophys.J. **850** (2017) L35, [arXiv:1710.05839]; IceCube collaboration [arXiv:1908.07706].

possibility and taking into account oscillations, the observations will then give precious information on the flavor composition in the production zone which in turn helps distinguish between production models<sup>86</sup>.

#### 14.6 Problems?

The three neutrino oscillation model can account, at present, for almost all data. However two collaborations, LSND<sup>87</sup> and MiniBooNE<sup>88</sup>, claim results in strong disagreement with the above experiments. To add to the confusion LSND results are not confirmed by KARMEN<sup>89</sup> where very similar technics are used. MiniBooNE considers  $\nu_{\mu} \rightarrow \nu_{e}$  and  $\overline{\nu}_{\mu} \rightarrow \overline{\nu}_{e}$  in short baseline experiments with  $.2 < E_{\nu}$  [GeV] < 1.25 and a ratio  $x/E_{\nu}$  in the range  $.25 < x/E_{\nu}$  [m/MeV] < 2.5. In a 2-neutrino oscillation model involving a sterile neutrino, the oscillations are best fitted with the parameters  $[\delta m^{2}, \sin^{2}(2\theta)] = [3.14 \text{ eV}^{2}, 0.002]$  for  $\nu$ 's, and  $[0.043 \text{ eV}^{2}, 0.88]$  for  $\overline{\nu}$ 's. MiniBooNE results are summarised saying that "the data are consistent with neutrino oscillations in the  $0.01 < \delta m^{2}$  [eV<sup>2</sup>] < 1.0 range" and they "have some overlap with the evidence for antineutrino oscillations from LSND".

In the last few years, the  $\overline{\nu}_e$  flux from nuclear reactors has raised a puzzle. In short baseline experiments (10 < x [m] < 100) there is a 6% deficit in the observed  $\overline{\nu}_e$  compared to model expectations: this is the Reactor Antineutrino Anomaly (RAA)<sup>90</sup>. Several explanations have been proposed. In a recent study the Daya Bay collaboration<sup>91</sup> observes correlations between the time evolution of the fuel in the core (the composition in U and Pu isotopes varies with time) and changes in the  $\overline{\nu}_e$  flux and energy spectrum. A detailed study of these correlations shows a 7.8% discrepancy between the observed and predicted  $^{235}$ U yields which suggests that this isotope is the main contributor to the RAA.

An alternative explanation has been to assume a fourth (sterile) neutrino to account for the  $\overline{\nu}_e$  deficit in short baseline nuclear reactor experiments. This is illustrated in Fig. 24 which shows that short and very short (less than 10 m) baseline reactor measurements are not sensitive to the three family neutrino parameters as given in eqs. (12.22), but would be affected by a fourth neutrino according the disappearance probability (see eq. (14.3)):

$$P(\overline{\nu}_e \to \overline{\nu}_e) = 1 - \sin^2(2\theta_{14}) \sin^2\left(\frac{x \,\delta m_{41}^2}{4 \,k}\right).$$

<sup>&</sup>lt;sup>86</sup>IceCube collaboration, M.G. Aartsen et. al., Astrophys.J. 809 (20158) 98, [arXiv:1507.03991].

 $<sup>^{87}</sup>$ LSND collaboration, A. Aguilar et al., Phys. Rev. **D64** (2001) 112007.

<sup>&</sup>lt;sup>88</sup>MiniBooNE collaboration, A. A. Aguilar-Arevalo, arXiv:1207.4809 [hep-ex]; Phys. Rev. Lett. **110** (2013) 161801; arXiv:1303.2588 [hep-ex].

<sup>&</sup>lt;sup>89</sup>KARMEN collaboration, B. Armbruster et al., Phys. Rev. **D65** (2002) 112001.

 $<sup>^{90}</sup>$ G. Mention et. al., Phys. Rev. **D83** (2011) 073006, arXiv:1101.2755 [hep-ex].

<sup>&</sup>lt;sup>91</sup>Daya Bay collaboration, F. P. An et. al., Phys. Rev. Lett. 118 (2017) 251801, arxiv:1704.01082 [hep-ex].

# Nouvelle oscillation vers un neutrino stérile?

 Pas de couplage par interaction faible →Visible uniquement par effet d'oscillation

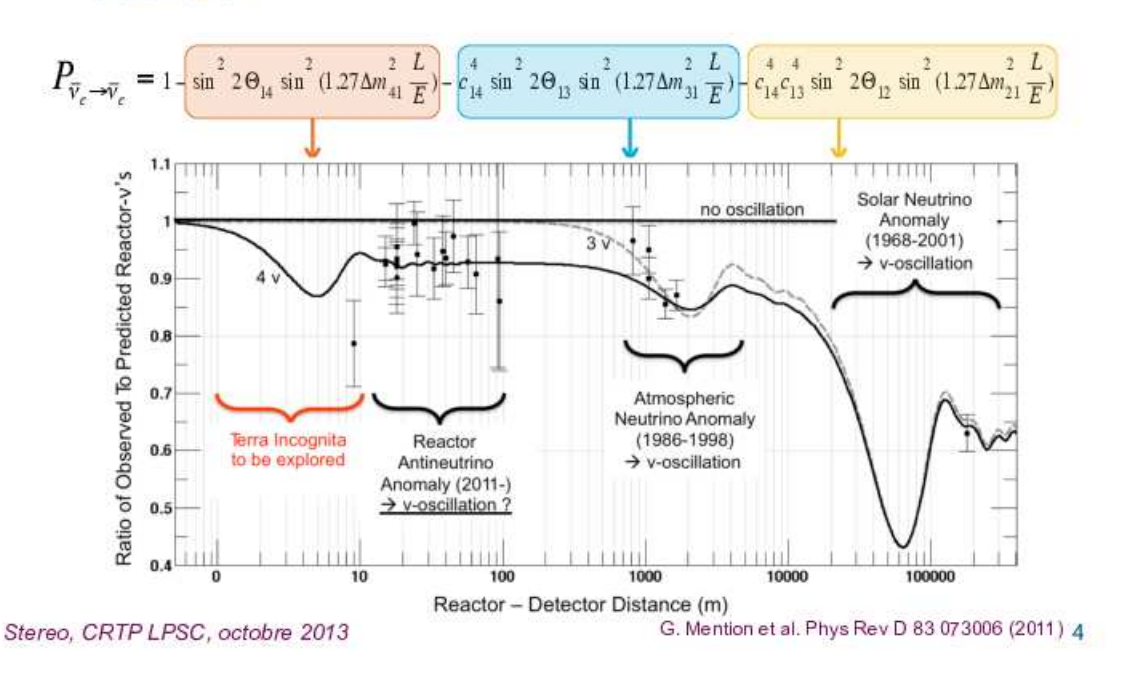


Figure 24: The figure illustrates the range of various oscillation parameters as a function the reactor-detector distance: a sterile neutrino with parameters as given in the text does not affect long base-line experiments, from the 2013 presentation of STEREO experiment by S. Kox et al., on the site lpsc.in2p3.fr/trac/neutrino/wiki/.

The best global fit<sup>92</sup> to short baseline  $\overline{\nu}_e$  disappearance is obtained with  $\delta m_{41}^2$  of the order of 1. eV<sup>2</sup> and  $\sin^2(2\theta_{14}) \approx .1$ . To further test the hypothesis of a sterile neutrino several experiments with very short baseline are taking data. DANSS<sup>93</sup> is located at a nuclear reactor in Russia with detectors at 10,7 m and 12,7 m from the core while the NEOS collaboration<sup>94</sup> has been taking data at a nuclear reactor in Korea at a distance of around 24 m from the core. More recently STEREO<sup>95</sup> at ILL

 $<sup>^{92}</sup>$ J. Kopp *et al*, JHEP 1305:050 (2013); see also C. Giunti, X. P. Ji, M. Laveder, Y. F. Li and B. R. Littlejohn, JHEP 1710 (2017) 143, arXiv:1708.01133 [hep-ph]; M. Dentler *et. al.*, JHEP 1711 (2017) 099, arxiv:1709.04294 [hep-ph].

 $<sup>^{93}</sup>$ DANSS collaboration, I. Alekseev *et. al.*, JINST **11** (2016) P11011, arXiv:1606.02896 [physics.ins-det]; arXiv:1804.04046 [hep-ex].

<sup>&</sup>lt;sup>94</sup>NEOS collaboration, Y.J. Ko et. al., Phys. Rev. Lett. 118 (2017) 121802, arXiv:1610.05134 [hep-ex].

<sup>&</sup>lt;sup>95</sup>STEREO collaboration, N. Allemandou, et. al., arXiv:1804.09052 [physics.ins-det]; Phys. Rev. Lett. 121 161801

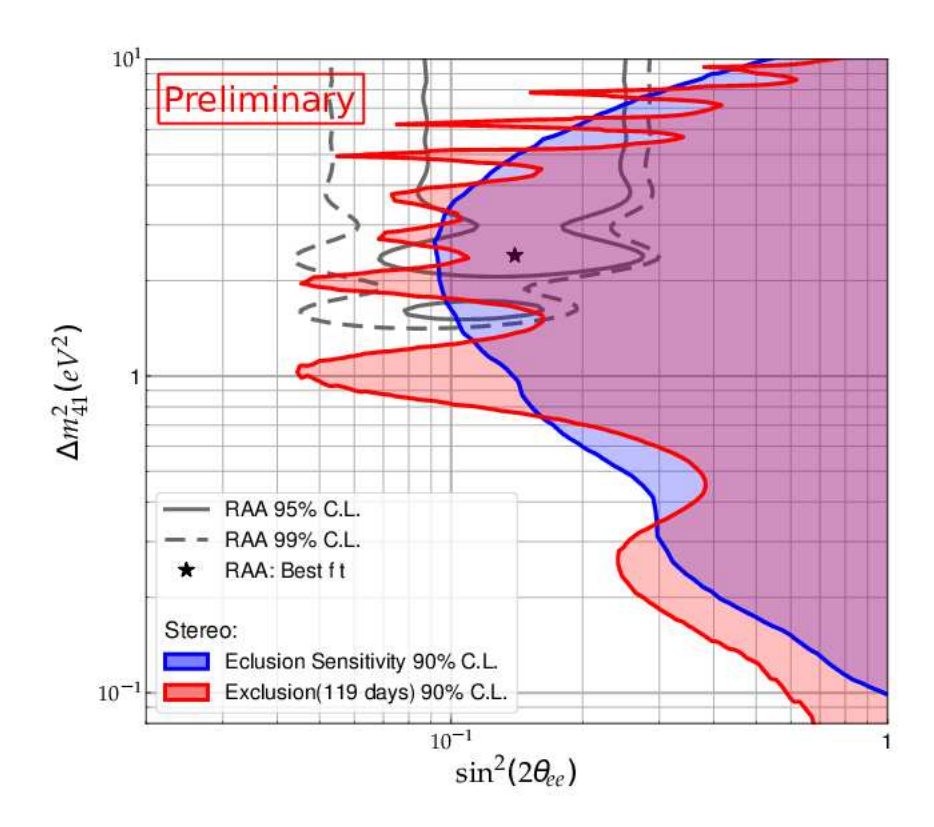


Figure 25: Exclusion contour in the parameter space  $\delta m_{41}^2, \sin^2(2\theta_{14}) \equiv \sin^2(2\theta_{ee})$ . The RAA contours are taken from G. Mention et al.<sup>90</sup> and the RAA best fit is marked by  $\bigstar$ . From STEREO publications<sup>95</sup>.

Grenoble, a high flux reactor using a 93% enriched  $^{235}\mathrm{U}$  with no time evolution on the  $\nu_e$  flux, has a segmented detector taking data at distances between 9 and 11 m from the core. In PROSPECT<sup>96</sup>, at the High Flux Isotope Reactor at Oak Ridge National Laboratory, the detector is 7.4 m from the core. All these experiments reduce the domain of sterile neutrino parameters obtained in previous reactor data<sup>90</sup> or global fits<sup>92</sup> and already exclude some best fits, as illustrated in Fig. 25 from the STEREO collaboration: the best RAA fit is already excluded at 99% C.L. More data are being accumulated and could reduce further the allowed domain of  $\theta_{14}$ ,  $\delta m_{41}^2$ .

#### 14.7 Neutrinos: conclusions

The work for more precision on the determination of neutrino oscillation parameters is continuing. The present experiments will increase the precision even more and this is crucial for the determination

<sup>(2018),</sup> arXiv:1806.02096 [hep-ex]; L. Bernard arXiv:1905.11896 [hep-ex]].

<sup>&</sup>lt;sup>96</sup>PROSPECT collaboration, J. Ashenfelter et al., arXiv:1809.02784 [hep-ex].

of the  $\mathcal{CP}$  violating phase. This will also help settle the ambiguity of the neutrino mass hierarchy. For example, recent global fits<sup>30</sup> indicate that normal hierarchy, in the 3- $\nu$  model, is favoured over inverted hierarchy at a 3 $\sigma$  level and the  $\mathcal{CP}$  phase is constrained at the same level by .87 <  $\delta/\pi$  < 1.94. There remains the ambiguity in the mixing angle  $\theta_{23}$  which is near the maximum mixing value ( $\sin(2\theta_{23}) \approx 1$ ), but in which octant ( $\theta_{23} \leq \pi/4$  or  $\theta_{23} \geq \pi/4$ )? Measuring these parameters with precision will be a long process: for example the DUNE collaboration<sup>97</sup> expects to measure  $\delta$  to better than 20° and

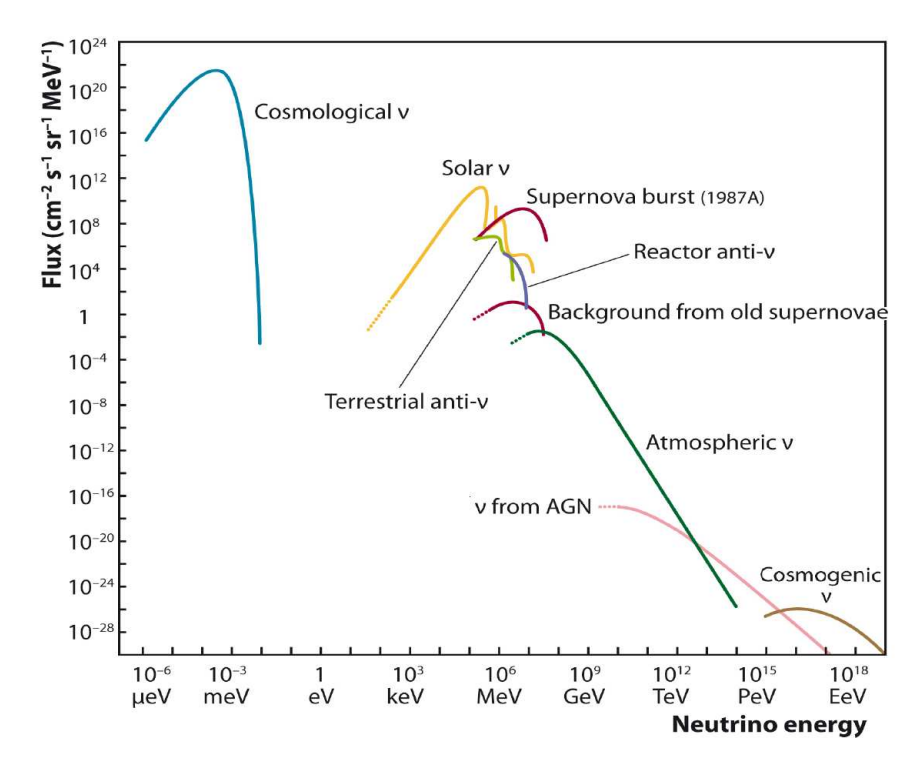


Figure 26: The measured or expected flux of neutrinos originating from different sources, from C. Spiering, Eur. Phys. J. **H37** (2012) 515, [arXiv:1207.4952]. The range in energy covers 24 orders of magnitude, from  $\mu eV$  to EeV

resolve the  $\theta_{23}$  octant with a 5  $\sigma$  significance after 10 years of running. The absolute mass scale of neutrinos is not settled yet although (model dependent) cosmological constraints become stronger and stronger. Also, are neutrinos of Dirac type or of Majorana type (see next section)? Finally there remains the question: are sterile neutrinos necessary? On this last topic progress is soon expected thanks to the future very short baseline reactor data. Despite these open questions, neutrinos are on the verge of becoming useful messengers which will contribute to the understanding of astrophysical

 $<sup>^{97}</sup>$  For the DUNE collaboration, N. Grant, PoS(NuFact2017) 052 (2017). DUNE is a long base line oscillation experiment (1300 km) with a highly pure  $\nu_{\mu}$  beam from FERMILAB and 4 10kt Liquid Argon Time Projection Chambers deep underground in South-Dakota, expected to start operation in 2026.

phenomena and objects such as gamma-ray bursts, supernovae remnants, quasars, blazars,  $\cdots$  <sup>98</sup>. As an illustration, in Fig. 26 is summarized in a semi-quantitative way the flux of neutrinos associated to different sources. Notice that there is more than 36 orders of magnitude between the solar neutrino flux and the expected cosmogenic flux.

Neutrinos may also be a signal of dark matter annihilation in the universe<sup>99</sup>.

 $<sup>^{98} \</sup>mathrm{Astro}2020$  Science White Paper: Cosmology and Fundamental Physics, K.N. Abazajian  $et~al.,~\mathrm{arXiv:}1903.04333,~[astro-ph].$ 

<sup>&</sup>lt;sup>99</sup>M. Chianese, arXiv:1907.11926, [hep-ph].